Journal of Theoretical Biology 449 (2018) 103–123

Contents lists available at ScienceDirect

Journal of Theoretical Biology

journal homepage: www.elsevier.com/locate/jtbi

Control in dormancy or eradication of cancer stem cells: Mathematical modeling and stability issues

Walid Djema[a,*], Catherine Bonnet[b], Frédéric Mazenc[b], Jean Clairambault[c], Emilia Fridman[d], Pierre Hirsch[e], François Delhommeau[e]

[a] Inria Saclay, CentraleSupélec, Université Paris-Saclay & Inria Sophia-Antipolis, Biocore and McTao teams, Université Côte d'Azur (UCA), France
[b] Inria Saclay, Disco team, Université Paris-Saclay, CentraleSupélec, L2S (CNRS), France
[c] Inria, Mamba team and Sorbonne Université, Paris 6, UPMC, Laboratoire Jacques-Louis Lions, Paris, France
[d] Department of Electrical Engineering and Systems at the School of Electrical Engineering, Tel-Aviv, Israel
[e] Sorbonne Université, GRC n7, Groupe de Recherche Clinique sur les Myéloproliférations Aiguës et Chroniques, AP-HP, Hôpital Saint-Antoine, Paris F-75012, France

ARTICLE INFO

Article history:
Received 11 September 2017
Revised 17 February 2018
Accepted 31 March 2018
Available online 17 April 2018

MSC:
93C23
93C10
93A30
93D05
92B05
92C50
80A30
37L15
39A30
39A60

Keywords:
Delay
Nonlinear
Lyapunov
Cancer dormancy
Modeling

ABSTRACT

Objective: Modeling and analysis of cell population dynamics enhance our understanding of cancer. Here we introduce and explore a new model that may apply to many tissues.

Analyses: An age-structured model describing coexistence between mutated and ordinary stem cells is developed and explored. The model is transformed into a nonlinear time-delay system governing the dynamics of healthy cells, coupled to a nonlinear differential-difference system describing dynamics of unhealthy cells. Its main features are highlighted and an advanced stability analysis of several steady states is performed, through specific Lyapunov-like functionals for descriptor-type systems.

Results: We propose a biologically based model endowed with rich dynamics. It incorporates a new parameter representing immunoediting processes, including the case where proliferation of cancer cells is locally kept under check by the immune cells. It also considers the overproliferation of cancer stem cells, modeled as a subpopulation of mutated cells that is constantly active in cell division. The analysis that we perform here reveals the conditions of existence of several steady states, including the case of cancer dormancy, in the coupled model of interest. Our study suggests that cancer dormancy may result from a plastic sensitivity of mutated cells to their shared environment, different from that – fixed – of healthy cells, and this is related to an action (or lack of action) of the immune system. Next, the stability analysis that we perform is essentially oriented towards the determination of sufficient conditions, depending on all the model parameters, that ensure either a regionally (i.e., locally) stable dormancy steady state or eradication of unhealthy cells. Finally, we discuss some biological interpretations, with regards to our findings, in light of current and emerging therapeutics. These final insights are particularly formulated in the paradigmatic case of hematopoiesis and acute leukemia, which is one of the best known malignancies for which it is always hard, in presence of a clinical and histological remission, to decide between cure and dormancy of a tumoral clone.

1. Introduction and overview of the objectives

1.1. Cancer stem cells (SCS): a unified hypothesis to all types of cancer

Stem cells (SCs) are undifferentiated cells characterized by their ability to self-renew and their multipotency, which is the ability to differentiate into more mature and specialized cells (Morgan, 2006; Tuch, 2006). A SC that engages in the division process undergoes successive transformations until becoming, at the end

* Corresponding author.
E-mail addresses: walid.djema@inria.fr (W. Djema), catherine.bonnet@inria.fr (C. Bonnet), frederic.mazenc@inria.fr (F. Mazenc), jean.clairambault@inria.fr (J. Clairambault), emilia@eng.tau.ac.il (E. Fridman), pierre.hirsch@aphp.fr (P. Hirsch), francois.delhommeau@aphp.fr (F. Delhommeau).

https://doi.org/10.1016/j.jtbi.2018.03.038
0022-5193/

of its cell cycle, two daughter cells. A heavy regulatory process controls committed cells before and during mitosis, by triggering a series of physiological events during the cycle. Even in fast-renewing tissues (e.g. gut, bone marrow and skin), cells are not always proliferating, but on the contrary, most of them are in a non-proliferating state, called resting or quiescent phase, G_0 (Morgan, 2006). Sometimes a pathological population of cells, that initially does not necessarily belong to the SC subpopulation, acquires self-renewing and proliferating capabilities similar to those of SCs (Enderling, 2013; Passegué et al., 2003). These stem-like cells are very often out of control (Reya et al., 2001) and they are capable of initiating, developing and regenerating cancers (Enderling, 2013), hence their designation as cancer stem cells (CSCs) (Jordan et al., 2006). Very often, CSCs are characterized by unhealthy behaviors such as excessive proliferation and loss of their differentiation faculties. This is what we observe for instance in the case of leukemia (Döhner et al., 2015). On the other hand, it cannot be disregarded that in some cases (as in breast cancer and leukemia, Al-Asadi et al., 2017; Ebinger et al., 2016) CSCs do not overproliferate (cancer without disease, Folkman and Kalluri, 2004, or, *in situ* tumor). However, even during their non-overproliferating states, CSCs remain in general distinguishable through specific markers on their surface[1] (Reya et al., 2001). In medical research, the CSC hypothesis[2] postulates that one subpopulation of cells holds the power of initiating and regenerating cancer (Enderling, 2013). This stemness property in non-SCs has been first observed in leukemia, then in many other types of cancer. Not surprisingly, the study of leukemic cells became a model for many other stem-like cells (Reya et al., 2001).

1.2. Evidences and underlying assumptions about cancer dormancy

Strong evidence about the existence of a stalled growth state, commonly referred to as *tumor dormancy*, has been established many years ago when microscopic tumors were frequently encountered during autopsy examinations (Folkman and Kalluri, 2004; Nielsen et al., 1987). The most likely explanations (see Aguirre-Ghiso, 2007; and also Folkman and Kalluri, 2004 and Schreiber et al., 2011) of CSCs dormancy state are: *(H.1)* blood and nutrient supply issues that prevent tumor growth, or at least delay its clinical manifestation (Naumov et al., 2009), and *(H.2)* vigilance of the immune system which, in some cases, suffices to stop tumor development (see Ferrarini et al., 2002; Naumov et al., 2009; Schreiber et al., 2011; Vesely, 2011; Wilkie and Hahnfeldt, 2013 and the references therein). In fact, there has been a lengthy debate on the role of the immune system in the defense against cancer: a process called *cancer immunosurveillance* (Vesely, 2011). The ambiguity about the immunosurveillance concept stems from the fact that often the immune system favors the development of the tumor instead of trying to eliminate it. The concept that attempts to integrate the diverse effects of the immune system on tumor progression is known as *cancer immunoediting* (see the review articles Schreiber et al., 2011 and Vesely, 2011). Even if it appears as an unsystematic process, an interest arises for cancer therapies that are immuno-oriented, bearing the name of *immunotherapy*.[3] In a similar spirit, monoclonal antibodies, e.g. gemtuzumab-ozogamicin, have been approved in the treatment protocols of some cancers (as in acute myeloid leukemia, Godwin et al., 2017), even if more trials are still needed to identify their exact benefits (Godwin et al., 2017; Rowe and Löwenberg, 2013). Other cancer therapies, sometimes assimilated to immunotherapy, are using some *immune checkpoint inhibitors* (see for instance, Brahmer and Pardoll, 2013; Langer, 2015; and Pardoll, 2012). In the last part of our work, we will be shortly adopting some of these immuno-oriented concepts, associated with classical chemotherapy or targeted therapies, as it is frequently adopted in practice. More generally, the complex link between the immune system and cancer dormancy (as it is summarized in Fig. 4 of Schreiber et al., 2011) is implicitly represented in our model thanks to an extra-parameter that we introduce, as detailed in the sequel (see Section 2.2).

1.3. Is cancer dormancy a promising therapeutic option?

In a general perspective, apart from the interpretation of tumor dormancy as an observed natural phenomenon in human cancers, the idea to transform cancer into a chronic disease is in the voices of many people in the medical world nowadays (Aguirre-Ghiso, 2006; Gatenby, 2009). Indeed, the interesting issue here is about: *how can we bring CSCs from an overproliferating activity to a dormant state?* More precisely, since cancer treatments most often consist of delivering the maximum tolerable doses of drugs in order to kill clinically apparent tumors, and knowing that an incompletely eradicated cancer frequently grows again, even more aggressively than the initial one (Enderling, 2013), the option of maintaining the tumor in dormancy is more appealing than trying to eradicate it (Jansen et al., 2015). Further discussions on the opportunities offered by cancer dormancy in therapeutics can be found for instance in Aguirre-Ghiso (2006), Gatenby (2009), Uhr et al. (1997) and the references therein.

The development of a relevant mathematical framework appears as a necessary tool to apprehend tumor dormancy as a biological mechanism (Kareva, 2016), with the ultimate goal to apply it in therapeutic settings. However, the task of mastering CSCs, i.e. bringing them into a dormant state, seems to be difficult to achieve. Indeed, one of the first dormancy-oriented therapeutic approaches in the case of solid tumors has not been very fruitful. It was based on the use of *angiogenesis inhibitors*[4] as drugs that choke off the blood supply of the tumor, in order to maintain it in dormancy. However, unexpected effects occurred in practice, and in some situations, targeting the blood vessels that feed tumors actually accelerated the spread of cancer (see Hayden, 2009; Reynolds, 2009). Therefore, it seems that tumor dormancy is more likely to be assigned to immuno-vigilance[5] (*H.2*), than to nutrient supply limitations (*H.1*). In light of the previously mentioned observations, one can say that dormancy has actually generated more issues than answers, in the process of understanding cancer. Among the open issues, we emphasize the following ones: *when a treatment protocol is elaborated for CSCs eradication with a given rate of success, how can we actually administer it (or a part of it) in order to achieve dormancy?* In addition, since eradication techniques may generate some surviving tumors which become even more aggressive than the initial ones, a key question is to determine *whether it is effective to consider the same targets and drugs, as for CSCs eradication, in order to achieve dormancy?* One can already figure out the utility of mathematical studies in such a context. Finally, we emphasize that, in the clinic of cancers today, eradication of CSCs re-

[1] For instance, stems cells in acute myeloid leukemia have some *interleukin-3receptor α chain* surface markers, which are not found in normal hematopoietic stems cells (see Feuring-Buske et al., 2002; Jordan et al., 2006).

[2] The reference as *CSC paradigm* has also gained ground recently. Several subpopulations of cells, with distinct cancer-initiating powers, form actually a tumor. One subpopulation has an indefinite potential of self-renewing and shows *stem-like* status. It appears also that *stemness* might be a transient cell state that is associated to epigenetic changes (Chaffer et al., 2011).

[3] Immunotherapy aims to help the immune system destroy cancer cells. It is given after – or at the same time as – another cancer treatment such as chemotherapy.

[4] These are substances that inhibit the growth of new blood vessels (Folkman and Kalluri, 2004).

[5] In particular, cancer dormancy results from the action of adaptive immunological mechanisms, through T cells, IL-12 and IFN-gamma (Schreiber et al., 2011).

mains the predominant treatment approach (although there is still a long way to improve the existing eradication treatment strategies, Stone et al., 2017).

1.4. Objectives of the study – particular insights into the hematopoietic system

We aim to provide a consistent theoretical framework for the modeling and the analysis of healthy and unhealthy cell dynamics, following different medical orientations, among which: the case where therapy aims to eradicate cancer cells while preserving healthy ones, and the scenario that consists in maintaining healthy and unhealthy cells in a controlled stable steady-state (i.e. cancer dormancy). To that purpose, a model of coexistence between ordinary and mutated cells is introduced and analyzed. Firstly, we investigate the stability properties of the trivial steady state of the resulting model: this is equivalent to the radical case in which all the cells are eradicated. Then, we perform a stability analysis that applies to cases of cancer dormancy and unhealthy cell eradication (while healthy cells survive). For the biological motivations stated in the above sections, we will focus on the study of cancer dormancy throughout our paper.

At this juncture, we express our keen interest in the hematopoietic system. We define hematopoiesis as the process initiated by the hematopoietic SC population inside the bone marrow, that leads to the formation and continuous replenishment of all the blood cells in the body (Hoffman et al., 2012). Hematopoiesis provides a model for studying and understanding all the mammalian stem cells and their niches (Crane et al., 2017), as well as all the mechanisms involved in the cell cycle, particularly cell differentiation. The hematopoietic paradigm is used in biology and medicine, as well as in the modeling and analysis of all similar processes. In Pujo-Menjouet (2016), the author reviewed the mathematical modeling of blood cell dynamics and its related pathological disorders within the past five decades. It is within this framework that we can situate our work, as a continuity of modeling and stability analysis of blood cell dynamics. However, as for the majority of works discussed in Pujo-Menjouet (2016), the models that we study can be used to cover other tissues and mechanisms. At this point, it is worth mentioning that pioneering works that formulated early blood cell dynamical models have been introduced for any type of cells (Smith and Martin, 1973), or borrowed from models describing other tissues, different from blood cell dynamics (see Burns and Tannock, 1970 for a dorsal epidermis cell model that inspired all the cell cycle models containing a resting phase). The interested reader is referred to Pujo-Menjouet (2016) for more information. Therefore, we emphasize in this study the paradigmatic case of hematopoietic SCs, which are at the root of the overall hematopoietic system. Hematopoietic SCs give rise to both the myeloid and lymphoid lineages of blood cells. The myeloid cells include many types of white blood cells (monocytes, macrophages, neutrophils, eosinophils), red blood cells (erythrocytes), and platelets (megakaryocytes). The hematopoietic process has to be well controlled (Hoffman et al., 2012) in order to avoid a wide range of blood disorders.[6] Acute myeloid leukemia (AML) is one of the most deadly blood malignancies. It affects the myeloid lineage and it is characterized by an overproliferation of abnormal immature white blood cells (blasts) of the myeloid lineage. Currently, AML treatment still relies on heavy chemotherapy with a high toxicity level and a low rate of success (Döhner et al., 2015). In fact, the only certain AML cure being not the result of chemotherapy, but of total bone marrow transplant that induces nearly 10–20% of mortality during the manipulation and due to severe reaction, GVH, of the graft versus the host. A better understanding of the behavior of CSCs (called leukemic cells in AML) should allow us to propose some selective combined targeted therapies that lead, theoretically, to cancer dormancy. In particular, our ambition is to provide a theoretical framework, taking into account observations made by hematologists, and allowing for the suggestion of insights into cancer treatments. It is in this light that we proposed in Djema et al. (2016b) a model of cohabitation between ordinary and mutated cells in the case of the hematopoietic system. The latter model follows recent observations (made in Hirsch et al., 2016 and in many other works) that associate the emergence of leukemic cells with an accumulation of several mutations, most often occurring in a standard chronological order (Hirsch et al., 2016), in the SC compartment. Thus, we have mathematically analyzed in Djema et al. (2016b, 2017b) two categories of heterogeneous cells as illustrated in Fig. 1 below, where the addition of mutations (on TET2, NPM1, FLT3) that we have considered had been established in Hirsch et al. (2016). We pursue in this work an analysis that provides a theoretical framework following different medical orientations, among which: (i) the case where therapy aims to eradicate cancer cells while preserving healthy cells, (ii) a less demanding, more realistic, scenario that consists in maintaining healthy and unhealthy cells in a controlled stable steady-state (cancer dormancy). Thus, our work extends the one that we proposed in Djema et al. (2016b, 2017b) and in a series of works: Adimy et al. (2015), Avila (2014), Avila et al. (2012), (but see also Adimy et al., 2008; Djema et al., 2017a; Foley et al., 2009; Fridman et al., 2016; Marciniak-Czochra et al., 2009; Özbay et al., 2012; Pujo-Menjouet et al., 2005; Stiehl and Marciniak-Czochra, 2011; Stiehl and Marciniak-Czochra, 2012). It is worth mentioning that the model in Avila et al. (2012) can neither model dormancy nor the abnormal overproliferation (e.g. invasion of the bone marrow by blasts). The latter point is improved by adopting a different form of fast self-renewing process, which has been recently introduced in Adimy et al. (2015), and where a subpopulation of cells is considered to be always active in proliferation (Adimy et al., 2015). In fact, cancer dormancy has not been considered in all the previously mentioned works. This is indeed a new area in cancer therapy (see Aguirre-Ghiso, 2006; Enderling, 2013; Jansen et al., 2015; Uhr et al., 1997) that we want to highlight here (but see also Kareva, 2016 for a different approach of modeling and analysis of cancer dormancy).

1.5. Organization of the work

In light of the above mentioned remarks, the coupled model (between healthy and mutated cells as in Fig. 1 below) of interest is presented in Section 2. Next, some features of the resulting coupled differential-difference model, together with the conditions of existence of our favorable steady states (reflecting dormancy and CSCs eradication), are discussed in Section 3. Then, in Section 4, the stability analysis of the case of all-cell extinction, via a construction of a linear Lyapunov-like functional, is performed (here we provide conditions for global exponential stability of the trivial steady state of the coupled model). Then, afterwards, we address in Section 5 the stability analysis, in the time-domain framework, of the cases describing cancer dormancy, and, unhealthy cells eradication (while healthy cells survive). The latter study goes through quadratic Lyapunov-like constructions (i.e. suitable degenerate functionals for the class of differential-difference systems). In fact, we are going to use two slightly different constructions: the first one is more general and relies on Linear Matrix Inequality (LMI) conditions derived via the *descriptor* method

[6] In particular, periodic diseases, such as cyclic neutropenia and some cases of chronic acute leukemia (see Bernard et al., 2003; Colijn and Mackey, 2005; Mackey et al., 2006; Pujo-Menjouet et al., 2005, and the references therein), but also overproliferating malignant hemopathies, such as acute myeloid leukemia (Adimy et al., 2008; Djema et al., 2016b; Özbay et al., 2012).

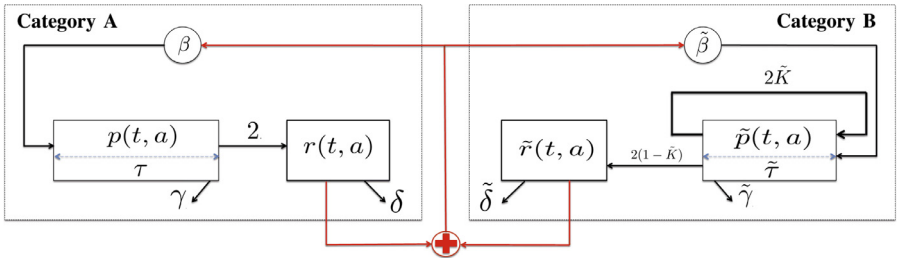

Fig. 1. Schematic representation of the coupled model of interest, involving a healthy SCs compartment (on the left) and an unhealthy compartment (on the right). For the sake of simplicity, we assume that unhealthy cells are those presenting mutations that lead to cancer. Indeed, we consider that abnormal stem cells (Category B) have for instance a first mutation in some genes encoding enzymes in epigenetics (e.g. on TET2, DNMT3A Delhommeau et al., 2009; Pronier and Delhommeau, 2011), that increases the self-renewing activity of the affected cells. A more serious pathological situation arises when a second mutation, affecting this time the pathways regulating the differentiation process such as NPM1 or transcription factors, appears on some of the cells. The superposition of these two events yields a blockade in differentiation. Finally, a subsequent mutation impairing proliferation control (e.g. FLT3-ITD) appears in a subpopulation of cells that have already accumulated one or more of the previously mentioned mutations. The latter event activates an uncontrolled overproliferation of a subpopulation of cells (CSCs) and thereby causes AML (Hirsch et al., 2016). Throughout this work, with a kind of abuse of notation, we use equivalently the designations: unhealthy cells, mutated cells, and CSCs. Similarly, healthy cells (Category A), or ordinary cells, represented on the left, are those which do not have any abnormal mutation, or those presenting some abnormalities which are not related to cancer. The definitions of the biological parameters (δ, $\tilde{\delta}$, γ, $\tilde{\gamma}$,...) are provided in Section 2.

(Fridman, 2014), applied to the linear approximation of the model around its nontrivial steady state of interest. This approach aims to provide a theoretical (sufficient) stability criterion, in the LMI form, to establish whether the steady state of a specific biological system is locally stable. The latter technique is followed by a second Lyapunov-type construction that allows us to determine *explicit* decay conditions (not in the LMI form) as well as an estimate of the decay rate of solutions and an approximation of the basin of attraction of the studied steady state. These sufficient stability conditions may be more restrictive than the LMI ones, however, they have the advantage of being easier to handle and, therefore, make it possible to interpret them biologically, from medical and therapeutic standpoints. Finally, numerical illustrations are provided and some concluding discussions, including biological interpretations of the findings, are outlined in Section 6.

2. A new general mathematical model involving coexistence between healthy and cancer stem cells

Our objective is to introduce a model more general than the existing ones, with regard to the recent biological features of interest, that are: cancer dormancy (Ebinger et al., 2016; Enderling, 2013), control and eradication of CSCs (Jansen et al., 2015). In particular, the compartment of unhealthy cells is hierarchized according to the severity of the mutations: cells that accumulate mutations up to that of FLT3 duplication (see Fig. 1) are constantly active in proliferation (as in Adimy et al., 2015). Our configuration allows us to reproduce and interpret the case of cancer dormancy, with the ultimate goal of providing theoretical stability conditions, along with therapeutic insights, that lead to stable dormant CSCs.

2.1. A multi-compartmental general model for healthy and unhealthy cells

We focus on the model illustrated in Fig. 1, where CSCs are characterized by an ability to over-proliferate represented by the parameter $\tilde{K}$ (in days^{-1}), as considered in Adimy et al. (2015), and previously envisaged in Avila et al. (2012) in a different configuration. More precisely, we notice that a subpopulation of unhealthy cells is in a permanent dividing state, namely the portion corresponding to $2\tilde{K}$, where, $0 < \tilde{K} < 1$ (as in Adimy et al., 2015 for a non-coupled model), which is different from the healthy SCs behavior (Fig. 1, on the left), where daughter cells, that arise from division of healthy mother cells, leave the proliferating compartment and join necessarily the resting one. Healthy resting stem cells can stay in G_0 until their death, differentiate, or start a new proliferating cycle by being transferred through the reintroduction function β to there proliferating compartment. Indeed, we mention that as many other works (see Adimy et al., 2008; Mackey, 1978; Pujo-Menjouet et al., 2005, among others), we are considering a compartmental model in which each cell can be in a resting phase or in a proliferating one. Finally, we mention that the coupled models studied in Avila et al. (2012), Djema et al. (2016b) do not admit a stable steady state that describes cancer dormancy, and this is an issue that we overcome here by considering a more general manner of coupling healthy and unhealthy SCs as discussed in the sequel.

Next, we denote by δ (resp. $\tilde{\delta}$) the rate, expressed in days^{-1}, of resting cells, which is lost either by differentiation or natural cell death for healthy SCs (resp. CSCs). A resting cell may start a cell cycle by entering in the proliferating phase during which each proliferating SC (resp. CSC) may die by apoptosis at a rate, expressed in days^{-1}, γ (resp. $\tilde{\gamma}$), or complete its mitosis and become two daughter cells at the end of the proliferating phase. We denote τ (resp. $\tilde{\tau}$) the average time (in days) taken to complete mitosis in the healthy (resp. unhealthy) proliferating compartment. For proliferation, the mechanisms regulating the entry into the cell cycle – at the cellular level – rely on some regulatory molecules that can play the role of growth factors (by stimulating the entry into proliferation of resting healthy and unhealthy cells), or, they can play the role of mitotic inhibitor ligands (meaning that mitosis proceeds normally if inhibitors are not combined with cell receptors, while it is stalled when they bind them). Consequently, we consider in our model that the transfer from the resting to the proliferating states is controlled by some reintroduction functions (as in Mackey, 1978; Pujo-Menjouet et al., 2005 and the majority of earlier works). More precisely, we let β (resp. $\tilde{\beta}$) be the reintroduction function from the healthy (resp. unhealthy) resting phase to the healthy (resp. unhealthy) proliferating phase. In addition, since healthy and unhealthy cells share the same environment (called *niches*, Crane et al., 2017 in hematopoiesis), we consider that each of the two functions β and $\tilde{\beta}$ depends simultaneously on both the total density of resting healthy cells, $x(t) = \int_0^\infty r(t,a)da$, and the total density of unhealthy resting cells, $\tilde{x}(t) = \int_0^\infty \tilde{r}(t,a)da$, where $r(t, a)$ and $\tilde{r}(t,a)$ are, respectively, the densities of resting healthy cells and resting unhealthy cells, of age $a \geq 0$, at time $t \geq 0$ (Djema et al., 2016b). This modeling approach reflects cohabitation between healthy and unhealthy cells, by considering that the entry into proliferation of healthy cells (resp. unhealthy cells) is also dependent on the total density of unhealthy cells (resp. healthy cells), the dynamics of the left and the right subpopulations in Fig. 1 becoming thus strongly coupled. Thus, the choice of the arguments

(i.e. coupling forms) given to the functions β and $\tilde{\beta}$ is crucial, since these arguments quantify the regulating mechanisms that affect healthy and unhealthy cells (see Mackey, 1978 for the case of non-coupled models).

2.2. The coupling form between ordinary and mutated cells

The functions β and $\tilde{\beta}$ represent the physiological inhibitory hormonal feedback by *Granulocyte Colony Stimulating Factors (G-CSF)* that is valid in the case of healthy as in the case of cancer cells. However, in the latter unhealthy situation, the sensitivity of the unhealthy cell population to this feedback may strongly vary. Now, the remaining issue regarding the functions β and $\tilde{\beta}$ is to select the coupling function between the total density of healthy resting cells x and the total density of mutated resting cells $\tilde{x}$ (i.e., to specify how β and $\tilde{\beta}$ actually depend on x and $\tilde{x}$). It appears that the simplest choice is to consider that both β and $\tilde{\beta}$ depend on the sum $x+\tilde{x}$, as previously considered in Avila et al. (2012) and Djema et al. (2016b). The latter scheme expresses a kind of absence of dominance between the populations x and $\tilde{x}$, since they show equal influence on β and $\tilde{\beta}$. However, differences actually exist between x and $\tilde{x}$ in their shared host – in particular immune – environment, mainly due to the mutations acquired by abnormal cells (Hollstein et al., 1991) and the reaction of the immune system. Changes that occur in mutated cell behavior may enhance the growth of cancer and result in cachexia and death (Bellomo and Forni, 1994) (see also Eftimie et al., 2011; Preziosi, 1996 for biological observations and modeling of the interaction between cancer and host environment). In our modeling approach, considering a coupling in the form $x+\tilde{x}$ means equal sensitivity of ordinary and mutated resting populations regarding the diverse proliferation regulation mechanisms, that act on the reintroduction of resting cells into proliferation. For example, due to epigenetic mutations, unhealthy cells may become less sensitive than healthy ones to the regulatory molecules secreted by the body and avoid the immune system (i.e. an immunosuppressive effect); on the other hand, healthy cells are in turn insensitive to the action of the immune system and less sensitive to drugs, since these drugs are designed to target unhealthy cells. In summary, healthy and unhealthy cells may react differently to their shared host environment (see Fig. 2 below), which may result in the dominance of one subpopulation (healthy or unhealthy), or possibly in cancer dormancy (Schreiber et al., 2011). Our first objective is to achieve a model that reproduces all these situations. Thus, we aim here to extend the modeling aspects by considering a more general form of coupling functions, so that some immunological effects can be represented. For that purpose, we consider that the argument of β is $x+\tilde{x}$, while $\tilde{\beta}$ depends at the same time on a weighted combination $x+\tilde{\alpha}\tilde{x}$, where $\tilde{\alpha}$ is some positive constant. We will show later in Section 3 that actually dormancy may be found mostly when $\tilde{\alpha}\neq 1$. In an illustrative manner, Fig. 2 provides a representation of the cases:

- $0\leq\tilde{\alpha}\leq 1$: even if ordinary and mutated cells are sharing the same environment, the mutated ones are less sensitive to the regulatory system present in the host environment, that may be identified as effects of the immune system on mutated cell proliferation. Consequently, unhealthy cells may escape a part of the regulatory system, including the immune system. This appears to be in line with medical practice, since the unhealthy behavior is mainly due to genetic/epigenetic mutations that make cells partially unresponsive to the regulating system. Consequently, the case $0\leq\tilde{\alpha}\leq 1$ suits well the untreated unhealthy behavior, in which cells avoid immune attacks and tend to get out of control, possibly leading to outgrowth of CSCs (Schreiber et al., 2011; Vesely, 2011; Zitvogel et al., 2006).

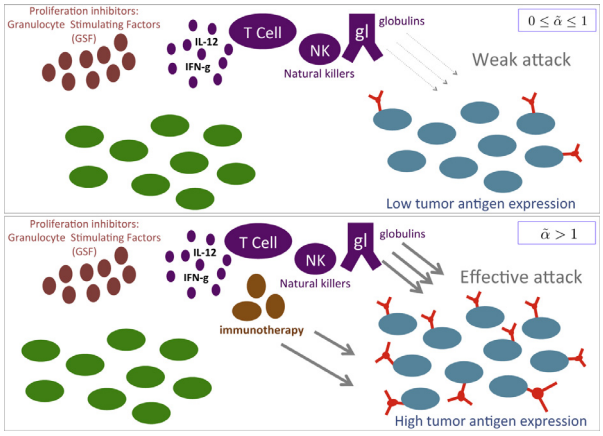

Fig. 2. Cartoon illustration of healthy and unhealthy cells in their shared environment. Ordinary SCs with normal behavior are in green, while mutated ones that go through quiescence to re-start a cell cycle (i.e. not the ones having the FLT3 mutation that makes them constantly active into proliferation) are in blue. The regulation of cell proliferation may include different mechanisms: release of growth factors and mitotic regulatory molecules, T cells, natural killers, globulins, IFN-g (IFN-gamma) and IL-12 (interleukin 12). Epigenetic mutations may also play a role on the way cells react to the whole regulating system. The case $0\leq\tilde{\alpha}\leq 1$ fits well a situation in which unhealthy cells are less sensitive to proliferation regulation than healthy ones. In this case, abnormal cells may hide their tumor antigens (an immunosuppressive state), which can be also due to the tumor variant cells that become no longer recognized and attacked by the adaptive immunity (Schreiber et al., 2011) and grow into insensitive cells to the entire immune effector mechanism. This condition is not enough in itself for the development of cancer, but it certainly favors it and may lead to the escape phase. On the other hand, the case $\tilde{\alpha}>1$ represents a situation in which proliferation of unhealthy cells is more controlled than the one of healthy cells. Reasons for this include an effective action carried out by the innate and adaptive immunity (sometimes this action suffices for total tumor eradication, see e.g. Vesely (2011) and Fig. 4 in Schreiber et al. (2011), but also the use of immunotherapy that acts in two ways: boosting the immune system to eliminate CSCs, and/or, enhancing the immune response by providing additional combative components such as reenabling exhausted T cells.

- $\tilde{\alpha}>1$: this case can describe an environment where unhealthy cells are more affected by the regulatory molecules than the healthy ones. This may be partly due to the effector response of the immune system (*cancer immunosurveillance*, Vesely, 2011), which may explain the dormancy phenomenon as a result of an efficient immune action that contains cancer growth (Wilkie and Hahnfeldt, 2013). In other words, the case $\tilde{\alpha}>1$ stands for a situation where proliferation of unhealthy cells may be locally kept under check by the immune system. This is the role of the innate and adaptive immunity which may lead to extrinsic tumor suppression in some rare cases, or to the adaptive immunity (T cells, IL-12, IFN-gamma) that at least may maintain cancer dormancy for long time (Schreiber et al., 2011).

Remark 1. A concept of dominance between healthy and mutated cells results from $\tilde{\alpha}$, that allows for an implicit representation of the immunologic mechanisms. In fact, what really makes the difference between cells is their respective sensitivity to the immune environment. The natural feedback represented by the functions β and $\tilde{\beta}$ depending on their arguments x and $\tilde{x}$, is in the case of cancer cells tuned by a sensitivity parameter $\tilde{\alpha}$ that may be seen as the faculty of unhealthy cells to over-express ($\tilde{\alpha}>1$) or hide ($\tilde{\alpha}<1$) their surface antigens.

In addition, it can also be argued that $\tilde{\alpha}>1$ relies on the use of drugs (immunotherapy, chemotherapy, etc.) that specifically target unhealthy cells. Indeed, we recall that immunotherapy mainly enhances the immune response, and that recent chemotherapy or targeted therapies are increasingly more accurate due to the over-expression of cancer receptors (which allow them to target unhealthy cells while the majority of healthy cells are spared). Finally,

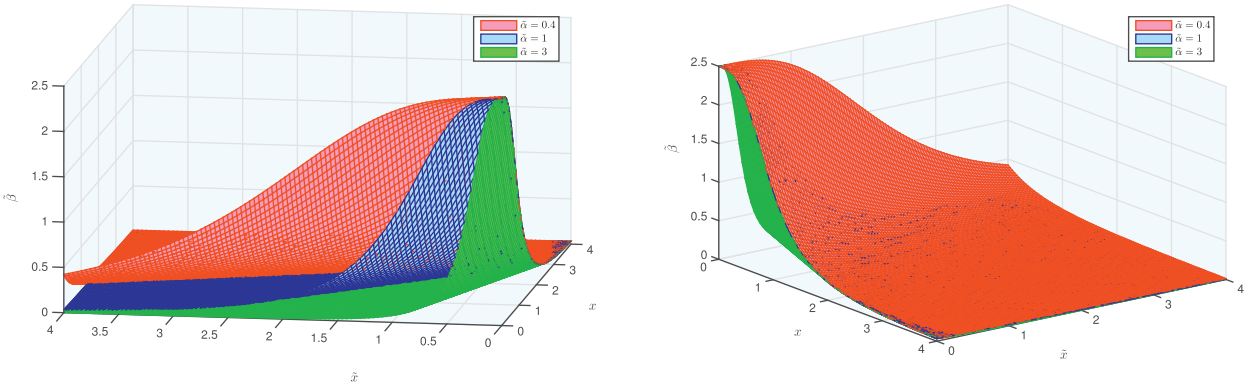

Fig. 3. Illustrative example of variations of a typical $\tilde{\beta}$-surface with respect to $\tilde{x}$ and x, for different values of $\tilde{\alpha}$ (i.e. in the three possible situations: $\tilde{\alpha} > 1$, $\tilde{\alpha} = 1$, and $\tilde{\alpha} < 1$).

we mention that the introduction of the above considerations related to the coupling functions between x and $\tilde{x}$ will make the dynamics of the resulting model richer than earlier models, as discussed in the next sections (Section 3). To the authors' knowledge, no equivalent model exists in the literature. Next, as conventionally considered, we assume that $\tilde{\beta}$ and β are nonlinear continuous decreasing functions, and, $\lim_{\ell\to\infty}\tilde{\beta}(\ell) = \lim_{\ell\to\infty}\beta(\ell) = 0$. As in Mackey (1978), Pujo-Menjouet et al. (2005), and all subsequent works for non-coupled models, we consider the typical Hill forms:

$$\tilde{\beta}(\ell) = \frac{\tilde{\beta}(0)}{1+\tilde{b}\ell^{\tilde{n}}}, \quad \beta(\ell) = \frac{\beta(0)}{1+b\ell^{n}} \tag{1}$$

where $\tilde{b}$, b, $\tilde{\beta}(0)$ and $\beta(0)$ are strictly positive real numbers and, $\tilde{n} \geq 2$ and $n \geq 2$. In fact, the Hill functions in (1), that belong to the family of functions with negative Schwarzian derivatives (see Ahsen et al., 2015, Chapter 3) are commonly encountered in many real-life problems. Classical arguments on cooperativity of enzyme inhibition kinetics (see Chapter 1 in Keener and Sneyd, 2009; and Qian, 2012), allow to determine the Hill-type expressions (1). The cooperative effect results in general from the fact that the binding of one regulatory molecule on one extracellular (surface) receptor of one cell will affect the binding of subsequent regulatory molecules on other receptors of the same cell. Due to the above considerations on the different sensitivities between healthy and unhealthy cells in the niches (1 and $\tilde{\alpha} \neq 1$, respectively), we can readily deduce that for given total densities x and $\tilde{x}$, the associated reintroduction functions β and $\tilde{\beta}$ actually operate according to:

$$\tilde{\beta}(x+\tilde{\alpha}\tilde{x}) = \frac{\tilde{\beta}(0)}{1+\tilde{b}(x+\tilde{\alpha}\tilde{x})^{\tilde{n}}}, \quad \beta(x+\tilde{x}) = \frac{\beta(0)}{1+b(x+\tilde{x})^{n}}. \tag{2}$$

2.3. Equations describing the dynamics of coupled cell populations

After the description of the particular case of the reintroduction functions β and $\tilde{\beta}$ according to the variation of the cell densities x and $\tilde{x}$ (as in Fig. 3), we now focus on the dynamical equations describing the populations of cells. Similarly to x and $\tilde{x}$, we denote by y and $\tilde{y}$, respectively, the total densities of proliferating healthy and unhealthy cells: $y(t) = \int_0^{\tau} p(t,a)da$, and, $\tilde{y}(t) = \int_0^{\tilde{\tau}} \tilde{p}(t,a)da$. The age-structured PDEs describing the coupled model in Fig. 1, are given for all $t > 0$ by:

$$\begin{cases} \partial_t\tilde{r}(t,a) + \partial_a\tilde{r}(t,a) = -\left[\tilde{\delta} + \tilde{\beta}(x,\tilde{x},\tilde{\alpha},t)\right]\tilde{r}(t,a), & a > 0, \\ \partial_t\tilde{p}(t,a) + \partial_a\tilde{p}(t,a) = -\tilde{\gamma}\,\tilde{p}(t,a), & 0 < a < \tilde{\tau}, \\ \partial_t r(t,a) + \partial_a r(t,a) = -[\delta + \beta(x,\tilde{x},t)]r(t,a), & a > 0, \\ \partial_t p(t,a) + \partial_a p(t,a) = -\gamma\, p(t,a), & 0 < a < \tau. \end{cases} \tag{3}$$

In McKendrick-type models (Foley et al., 2009; McKendrick, 1925; Wake, 2003), we observe that only the death rates (δ, $\tilde{\delta}$, γ and $\tilde{\gamma}$), and the removal terms (β and $\tilde{\beta}$, since the reintroduction functions are considered as cell loss from resting cells) appear in the PDE system (3). On the other hand, the new births, which are the renewal conditions at the age $a = 0$, for resting and proliferating cells, are introduced through the following boundary conditions:

$$\begin{cases} \tilde{r}(t,0) = 2(1-\tilde{K})\tilde{p}(t,\tilde{\tau}), \\ \tilde{p}(t,0) = \tilde{\beta}(x,\tilde{x},\tilde{\alpha},t)\tilde{x}(t) + 2\tilde{K}\tilde{p}(t,\tilde{\tau}) \triangleq \tilde{u}(t), \\ r(t,0) = 2p(t,\tau), \\ p(t,0) = \beta(x,\tilde{x},t)x(t), \end{cases} \tag{4}$$

for all $t > 0$, and where $\tilde{u}(t)$ represents the density of new proliferating unhealthy cells at time $t > 0$ (Adimy et al., 2015). Finally, the initial age-distributions, respectively, $\tilde{r}(0,a) = \tilde{r}_0(a)$, for $a > 0$, $\tilde{p}(0,a) = \tilde{p}_0(a)$, for $0 < a < \tilde{\tau}$, $r(0,a) = r_0(a)$, for $a > 0$, and $p(0,a) = p_0(a)$, for $0 < a < \tilde{\tau}$, are assumed to be L^1-functions.

Now, inspired by an illustrative approach in Thieme (2003), we give a biological explanation of the method of characteristics in our context. To avoid redundancy, we focus only on the unhealthy compartment. Let us define $\mathfrak{p}^*(a,s)$ as the density of unhealthy proliferating cells, of age a, that entered to the unhealthy proliferating phase at time s. This coincides with the density of unhealthy proliferating cells at time $t = a + s$ (Thieme, 2003). In other words, $\mathfrak{p}^*(a,s) = \tilde{p}(a+s,a)$. Therefore,

$$\frac{\partial\mathfrak{p}^*(a,s)}{\partial a} = \frac{\partial\tilde{p}(t,a)}{\partial t}\bigg|_{t=a+s} + \frac{\partial\tilde{p}(t,a)}{\partial a}\bigg|_{t=a+s} = -\tilde{\gamma}\mathfrak{p}^*(a,s).$$

It follows that $\mathfrak{p}^*(a,s) = \mathfrak{p}^*(0,s)e^{-\tilde{\gamma}a}$, where $\mathfrak{p}^*(0,s) = \tilde{p}(s,0)$.

Now, let us recover $\tilde{p}$ from $\mathfrak{p}^*$ (Thieme, 2003). Noticing that $\tilde{p}(t,a) = \mathfrak{p}^*(a,t-a)$, for $t > a$, we obtain, $\tilde{p}(t,a) = e^{-\tilde{\gamma}a}\tilde{p}(t-a,0)$, for all $t > a$.

Next, we define $\mathfrak{p}^{\mathfrak{v}}(t,s) = \tilde{p}(t,t+s)$, which can be interpreted as the density of unhealthy proliferating cells that are in the proliferating phase at time t, and have been in the proliferating phase at time 0, with an age $a = s$ at $t = 0$. Arguing as for $\mathfrak{p}^*$ (Thieme, 2003), we find that $\frac{\partial\mathfrak{p}^{\mathfrak{v}}(t,s)}{\partial t} = -\tilde{\gamma}\mathfrak{p}^{\mathfrak{v}}(t,s)$.

Then, $\mathfrak{p}^{\mathfrak{v}}(t,s) = \mathfrak{p}^{\mathfrak{v}}(0,s)e^{-\tilde{\gamma}t}$, where $\mathfrak{p}^{\mathfrak{v}}(0,s) = \tilde{p}(0,s) = \tilde{p}_0(s)$. Recovering $\tilde{p}$ from $\mathfrak{p}^{\mathfrak{v}}$, for $a \geq t$, gives us $\tilde{p}(t,a) = e^{-\tilde{\gamma}t}\tilde{p}_0(a-t)$, for all $a \geq t$.

We deduce that we have recovered the well-known solution (Thieme, 2003):

$$\tilde{p}(t,a) = \begin{cases} e^{-\tilde{\gamma}t}\tilde{p}_0(a-t), & 0 \leq t \leq a \\ e^{-\tilde{\gamma}a}\tilde{p}(t-a,0), & t > a. \end{cases} \tag{5}$$

Consequently, the first equation in (4) is then equivalent to

$$\tilde{r}(t,0) = \begin{cases} 2(1-\tilde{K})e^{-\tilde{\gamma}t}\tilde{p}_0(\tilde{\tau}-t), & 0 \leq t \leq \tilde{\tau}, \\ 2(1-\tilde{K})e^{-\tilde{\gamma}\tilde{\tau}}\tilde{p}(t-\tilde{\tau},0), & t > \tilde{\tau}. \end{cases} \tag{6}$$

From biological considerations we set, $\lim_{a\to\infty}\tilde{r}(t,a)=\lim_{a\to\infty} r(t,a)=0$, for all fixed value of $t\geq 0$. Then, using (8), and by integrating the first equation in (3) with respect to a between 0 and $+\infty$, we determine that the long time behavior (Bélair et al., 1995) of $\tilde{x}$ is given by $\dot{\tilde{x}}(t)=-(\tilde{\delta}+\tilde{\beta}(x,\tilde{x},\tilde{\alpha},t))\tilde{x}(t)+2(1-\tilde{K})e^{-\tilde{\gamma}\tilde{\tau}}\tilde{u}(t-\tilde{\tau})$, where we recall that the density $\tilde{u}(t)$ is the one defined in (4), and represents for all $t>0$ the density of new unhealthy proliferating cells. Similarly, by integrating the second equation in (3) over the variable a, between 0 and $\tilde{\tau}$, and using $\tilde{p}(t,\tilde{\tau})=\tilde{u}(t-\tilde{\tau})$, we get $\dot{\tilde{y}}(t)=-\tilde{\gamma}\tilde{y}(t)+\tilde{\beta}(x,\tilde{x},\tilde{\alpha},t)\tilde{x}(t)-(1-2\tilde{K})e^{-\tilde{\gamma}\tilde{\tau}}\tilde{u}(t-\tilde{\tau})$. Similarly, we can check that for the healthy compartment, we obtain for all $t>0$:

$$p(t,a)=\begin{cases}e^{-\gamma t}p_0(a-t), & 0\leq t\leq a\\ e^{-\gamma a}p(t-a,0), & t>a.\end{cases} \tag{7}$$

It follows that the third equation in (4) is then equivalent to:

$$r(t,0)=\begin{cases}2e^{-\gamma t}p_0(\tau-t), & 0\leq t\leq \tau,\\ 2e^{-\gamma\tau}p(t-\tau,0), & t>\tau,\end{cases} \tag{8}$$

where $p(t-\tau,0)$ is deduced from the fourth equation in (4). Thus, using similar arguments as for the unhealthy compartment, we deduce the following overall system for all $t>0$,

$$\begin{cases}\dot{\tilde{x}}(t)=-\left[\tilde{\delta}+\tilde{\beta}(x,\tilde{x},\tilde{\alpha},t)\right]\tilde{x}(t)+2(1-\tilde{K})e^{-\tilde{\gamma}\tilde{\tau}}\tilde{u}(t-\tilde{\tau}),\\ \dot{\tilde{y}}(t)=-\tilde{\gamma}\tilde{y}(t)+\tilde{\beta}(x,\tilde{x},\tilde{\alpha},t)\tilde{x}(t)-(1-2\tilde{K})e^{-\tilde{\gamma}\tilde{\tau}}\tilde{u}(t-\tilde{\tau}),\\ \tilde{u}(t)=\tilde{\beta}(x,\tilde{x},\tilde{\alpha},t)\tilde{x}(t)+2\tilde{K}e^{-\tilde{\gamma}\tilde{\tau}}\tilde{u}(t-\tilde{\tau}),\\ \dot{x}(t)=-[\delta+\beta(x,\tilde{x},t)]x(t)+2e^{-\gamma\tau}\beta(x,\tilde{x},t-\tau)x(t-\tau),\\ \dot{y}(t)=-\gamma y(t)+\beta(x,\tilde{x},t)x(t)-e^{-\gamma\tau}\beta(x,\tilde{x},t-\tau)x(t-\tau).\end{cases} \tag{9}$$

We notice that the dynamics of x, $\tilde{x}$ and $\tilde{u}$ do not depend on y and $\tilde{y}$. This (triangular) system structure leads us to study first:

$$\begin{cases}\dot{\tilde{x}}(t)=-\left[\tilde{\delta}+\tilde{\beta}(x(t)+\tilde{\alpha}\tilde{x}(t))\right]\tilde{x}(t)+2(1-\tilde{K})e^{-\tilde{\gamma}\tilde{\tau}}\tilde{u}(t-\tilde{\tau}),\\ \tilde{u}(t)=\tilde{\beta}(x(t)+\tilde{\alpha}\tilde{x}(t))\tilde{x}(t)+2\tilde{K}e^{-\tilde{\gamma}\tilde{\tau}}\tilde{u}(t-\tilde{\tau}),\\ \dot{x}(t)=-[\delta+\beta(x(t)+\tilde{x}(t))]x(t)+2e^{-\gamma\tau}\beta\\ (x(t-\tau)+\tilde{x}(t-\tau))x(t-\tau).\end{cases} \tag{10}$$

We can prove that a unique piecewise continuous solution, $(\tilde{x}(t),\tilde{u}(t),x(t))$, exists for all $t\geq 0$, when system (10) is associated with appropriate initial conditions $(\varphi_{\tilde{x}},\varphi_{\tilde{u}},\varphi_x)$, where, $\varphi_{\tilde{x}}\in\mathcal{C}([-\tau,0],\mathbb{R})$, $\varphi_x\in\mathcal{C}([-\tau,0],\mathbb{R})$, and, $\varphi_{\tilde{u}}\in\mathcal{C}([-\tilde{\tau},0],\mathbb{R})$. Moreover, we can show that the system (10) is positive, since $\tilde{K}\in(0,1)$. Throughout this work, only positive solutions of (10) are considered.

3. Notable features of the coupled model

In this section, we point out some properties of the model (10) that highlight its rich dynamics, according to the following possibly existing cases:[7]

Point of interest of $\tilde{x}$	0	$\tilde{x}_e$	0	$\tilde{x}_e$	$+\infty$
Point of interest of $\tilde{u}$	0	$\tilde{u}_e$	0	$\tilde{u}_e$	$+\infty$
Point of interest of x	0	0	x_e	x_e	*

• Cell extinction: clearly, (0, 0, 0), is an equilibrium point of model (10). Biologically, convergence to zero is synonymous of the extinction of all the cells (both healthy and unhealthy populations). From a therapeutic standpoint, we said that we aim to address theoretical studies for the case of unhealthy cells eradication (while ensuring that healthy cells survive), and also for a dormancy steady state (where all the cells are in a stable steady state). In both situations we do not want that healthy cells vanish. However, chemotherapy always affects – to a certain extent – healthy cells. But side effects of recent chemotherapy treatments are fewer than those of the drugs used in the past, since novel molecules (targeted therapies) are designed to target overexpressed receptors corresponding to mutated cells (i.e. drugs are more accurate since they attack cells with specific extracellular receptors expressed only on mutated cells). In addition, medications are mainly acting on cells during their phase of proliferation, while it appears that most of the healthy cells are in quiescence. Therefore, we consider that only a *radical* therapy will lead to total cell eradication, and this is a situation that we want to avoid. Nevertheless, the theoretical conditions, depending on the biological functions and parameter involved in our model, that cause total cell eradication are discussed in Section 4.

• Escape from dormancy in diseased cells: one of the main concerns related to dormancy is to explain how escape from tumor dormancy can emerge (see Kareva, 2016 and the non-coupled model in Adimy et al., 2015 that admits unbounded solutions). Similarly to Adimy et al. (2015), we notice in the coupled model (10) that the CSC-compartment may have unbounded solutions that reproduce the unlimited cell proliferation in cancer. Indeed, from the second equation in (10) it is obvious that $2\tilde{K}e^{-\tilde{\gamma}\tilde{\tau}}>1$, implies that, $\lim_{t\to+\infty}\tilde{u}(t)=+\infty$. It follows from the first equation in (10) that $\lim_{t\to+\infty}\tilde{x}(t)=+\infty$. This situation may reflect the escape from tumor dormancy, or the invasion of the bone marrow by the blasts as in AML.

• Existence of the desired steady states $\mathfrak{D}$ and $\mathfrak{E}$: let us start from the general case in which the point $(\tilde{x}_e,\tilde{u}_e,x_e)$ is a nonnegative steady state of (10). Therefore, it follows that this equilibrium point satisfies:

$$\begin{cases}\left[\tilde{\delta}+\tilde{\beta}(x_e+\tilde{\alpha}\tilde{x}_e)\right]\tilde{x}_e=2(1-\tilde{K})e^{-\tilde{\gamma}\tilde{\tau}}\tilde{u}_e,\\ \tilde{\beta}(x_e+\tilde{\alpha}\tilde{x}_e)\tilde{x}_e=\left(1-2\tilde{K}e^{-\tilde{\gamma}\tilde{\tau}}\right)\tilde{u}_e,\\ [\delta-(2e^{-\gamma\tau}-1)\beta(x_e+\tilde{x}_e)]x_e=0,\end{cases} \tag{11}$$

where we exclude the previously discussed case of unbounded solutions by assuming that: $2\tilde{K}e^{-\tilde{\gamma}\tilde{\tau}}<1$. Indeed, our main objective here is to determine necessary and sufficient conditions for the existence of $\mathfrak{D}=(\tilde{x}_e,\tilde{u}_e,x_e)$, where $x_e>0$, $\tilde{x}_e>0$ and $\tilde{u}_e>0$, and for the existence of $\mathfrak{E}=(0,0,x_e)$, where $x_e>0$.

First, since β is continuous and decreasing from $\beta(0)$ to zero, we deduce from the third equation in (11) that,

$$\delta<\left[2e^{-\gamma\tau}-1\right]\beta(0), \tag{12}$$

is a necessary and sufficient condition for the existence of x_e and $\tilde{x}_e$ such that, $x_e+\tilde{x}_e>0$, and, $\delta-(2e^{-\gamma\tau}-1)\beta(x_e+\tilde{x}_e)=0$. In fact, the inequality (12) is a necessary and sufficient condition for the existence of $\mathfrak{E}$ (but not $\mathfrak{D}$).

Next, from the second equation in (11), we obtain that $\tilde{u}_e=\frac{\tilde{\beta}(x_e+\tilde{\alpha}\tilde{x}_e)\tilde{x}_e}{1-2\tilde{K}e^{-\tilde{\gamma}\tilde{\tau}}}$.

By substituting $\tilde{u}_e$ in the first equation of (11), we get:

$$\left[\tilde{\delta}-\frac{2e^{-\tilde{\gamma}\tilde{\tau}}-1}{1-2\tilde{K}e^{-\tilde{\gamma}\tilde{\tau}}}\tilde{\beta}(x_e+\tilde{\alpha}\tilde{x}_e)\right]\tilde{x}_e=0. \tag{13}$$

The fact that $\tilde{\beta}$ is continuous and decreasing implies that the condition,

$$\tilde{\delta}<\left[\frac{2e^{-\tilde{\gamma}\tilde{\tau}}-1}{1-2\tilde{K}e^{-\tilde{\gamma}\tilde{\tau}}}\right]\tilde{\beta}(0), \tag{14}$$

is necessary and sufficient for the existence of x_e and $\tilde{x}_e$, such that, $x_e+\tilde{\alpha}\tilde{x}_e>0$, and, $\tilde{\delta}-\frac{2e^{-\tilde{\gamma}\tilde{\tau}}-1}{1-2\tilde{K}e^{-\tilde{\gamma}\tilde{\tau}}}\tilde{\beta}(x_e+\tilde{\alpha}\tilde{x}_e)=0$. Obviously, we notice that, $2\tilde{K}e^{-\tilde{\gamma}\tilde{\tau}}<1<2e^{-\tilde{\gamma}\tilde{\tau}}$. In fact, the condition (14) is a necessary and sufficient condition for the existence of $(\tilde{x}_e,\tilde{u}_e,0)$, where $\tilde{x}_e>0$ and $\tilde{u}_e>0$.

[7] Here we are considering that $\tilde{x}_e>0$, $\tilde{u}_e>0$ and $x_e>0$. We can notice that $\tilde{x}_e=0$ implies that $\tilde{u}_e=0$, and vice versa.

It is worth mentioning that, if the condition (12) is satisfied (i.e. the necessary and sufficient condition for the existence of $\mathfrak{E}$), together with the condition

$$\tilde{\delta} > \left[\frac{2e^{-\tilde{\gamma}\tilde{\tau}}-1}{1-2\tilde{K}e^{-\tilde{\gamma}\tilde{\tau}}}\right]\tilde{\beta}(0), \tag{15}$$

then (0, 0, 0) and $\mathfrak{E}$ are the unique existing steady states of the studied model. Let us now focus on the case where both x_e and $\tilde{x}_e$ are simultaneously strictly positive (and then $\tilde{u}_e$ is strictly positive). In the latter situation, we get,

$$\begin{cases} x_e + \tilde{\alpha}\tilde{x}_e = \tilde{\beta}^{-1}(\tilde{\mu}), \\ x_e + \tilde{x}_e = \beta^{-1}(\mu), \end{cases} \tag{16}$$

where, $\mu = \frac{\delta}{2e^{-\gamma\tau}-1}$, and, $\tilde{\mu} = \frac{\tilde{\delta}(1-2\tilde{K}e^{-\tilde{\gamma}\tilde{\tau}})}{2e^{-\tilde{\gamma}\tilde{\tau}}-1}$. Consequently, we get,

$$\begin{cases} x_e = \frac{1}{\tilde{\alpha}-1}\left[\tilde{\alpha}\beta^{-1}(\mu) - \tilde{\beta}^{-1}(\tilde{\mu})\right], \\ \tilde{x}_e = \frac{1}{\tilde{\alpha}-1}\left[\tilde{\beta}^{-1}(\tilde{\mu}) - \beta^{-1}(\mu)\right], \\ \tilde{u}_e = \frac{\tilde{\delta}}{2e^{-\tilde{\gamma}\tilde{\tau}}-1}\tilde{x}_e. \end{cases} \tag{17}$$

Now, we distinguish between the following two situations:

The case $\tilde{\alpha} = 1$: Here we notice that,

$$\begin{cases} x_e + \tilde{x}_e = \tilde{\beta}^{-1}(\tilde{\mu}) = \beta^{-1}(\mu), \\ \tilde{u}_e = \frac{\tilde{\delta}}{2e^{-\tilde{\gamma}\tilde{\tau}}-1}\tilde{x}_e, \end{cases} \tag{18}$$

which is either an impossible case if the biological parameters are such that $\tilde{\beta}^{-1}(\tilde{\mu}) \neq \beta^{-1}(\mu)$, or, when $\tilde{\beta}^{-1}(\tilde{\mu}) = \beta^{-1}(\mu)$, it corresponds to a *continuum* equilibrium point (the infinite possible values of x_e and $\tilde{x}_e$ that satisfy the first equation in (18)). We want to avoid the latter continuum equilibrium points since that case has no concrete biological signification.

The case $\tilde{\alpha} > 1$ or $\tilde{\alpha} < 1$: first, we focus on the case $0 < \tilde{\alpha} < 1$. We recall from earlier discussion that, biologically, $0 < \tilde{\alpha} < 1$ means that CSCs are less sensitive than ordinary cells to their shared environment composed by regulatory mitotic molecules (due to epigenetic mutations for instance, unhealthy cells no longer respond to inhibitory signals and continue to proliferate). More generally, $\tilde{\alpha} < 1$ plays the role of a mitigating factor of the effect of regulatory molecules that attenuate the entrance frequency into proliferation. Now, from (17), we deduce that a sufficient condition for the existence of $\mathfrak{D}$ when $\tilde{\alpha} < 1$, is given by: $\tilde{\alpha}\beta^{-1}(\mu) < \tilde{\beta}^{-1}(\tilde{\mu}) < \beta^{-1}(\mu)$.

On the other hand, we observe that when $\tilde{\alpha} > 1$, then, from (17), we deduce that a sufficient condition for the existence of $\mathfrak{D}$ is given by: $\beta^{-1}(\mu) < \tilde{\beta}^{-1}(\tilde{\mu}) < \tilde{\alpha}\beta^{-1}(\mu)$. We summarize the overall discussion in the following result:

Proposition 1. *(i) For all $\tilde{\alpha} > 0$, if the conditions*

$$\tilde{\delta} > \left[\frac{2e^{-\tilde{\gamma}\tilde{\tau}}-1}{1-2\tilde{K}e^{-\tilde{\gamma}\tilde{\tau}}}\right]\tilde{\beta}(0), \quad \text{and,} \quad \delta > \left[2e^{-\gamma\tau}-1\right]\beta(0), \tag{19}$$

are satisfied, then (0, 0, 0) is the unique equilibrium point of the system (10). Note that in fact (0, 0, 0) is always a steady state of the system (10).

(ii) For all $\tilde{\alpha} > 0$, the condition

$$\delta < \left[2e^{-\gamma\tau}-1\right]\beta(0), \tag{20}$$

is a necessary and sufficient conditions for the existence of the steady state, $\mathfrak{E} = (0, 0, x_e)$, where $x_e > 0$, for the system (10).

(iii) For all $\tilde{\alpha} > 0$, if the conditions

$$\tilde{\delta} > \left[\frac{2e^{-\tilde{\gamma}\tilde{\tau}}-1}{1-2\tilde{K}e^{-\tilde{\gamma}\tilde{\tau}}}\right]\tilde{\beta}(0), \quad \text{and,} \quad \delta < \left[2e^{-\gamma\tau}-1\right]\beta(0), \tag{21}$$

are satisfied, then (0, 0, 0) and $\mathfrak{E} = (0, 0, x_e)$ are the unique steady states of system (10).

(iv) For all $\tilde{\alpha} > 0$, the condition

$$\tilde{\delta} < \left[\frac{2e^{-\tilde{\gamma}\tilde{\tau}}-1}{1-2\tilde{K}e^{-\tilde{\gamma}\tilde{\tau}}}\right]\tilde{\beta}(0), \tag{22}$$

is a necessary and sufficient condition for the existence of the steady state $(\tilde{x}_e, \tilde{u}_e, 0)$ where, $\tilde{x}_e > 0$ and $\tilde{u} > 0$, for the system (10).

(v) For all $\tilde{\alpha} > 0$, if the conditions

$$\tilde{\delta} < \left[\frac{2e^{-\tilde{\gamma}\tilde{\tau}}-1}{1-2\tilde{K}e^{-\tilde{\gamma}\tilde{\tau}}}\right]\tilde{\beta}(0), \quad \text{and,} \quad \delta > \left[2e^{-\gamma\tau}-1\right]\beta(0), \tag{23}$$

are satisfied, then (0, 0, 0) and $(\tilde{x}_e, \tilde{u}_e, 0)$ are the unique steady states of system (10).

(vi) For all $\tilde{\alpha} > 0$, the conditions

$$\tilde{\alpha} \neq 1, \quad \tilde{\delta} < \left[\frac{2e^{-\tilde{\gamma}\tilde{\tau}}-1}{1-2\tilde{K}e^{-\tilde{\gamma}\tilde{\tau}}}\right]\tilde{\beta}(0), \quad \text{and,} \quad \delta < \left[2e^{-\gamma\tau}-1\right]\beta(0), \tag{24}$$

are necessary, but not sufficient, for the existence of $\mathfrak{D} = (\tilde{x}_e, \tilde{u}_e, x_e)$.

(vii) We denote $\mu = \frac{\delta}{2e^{-\gamma\tau}-1}$, and, $\tilde{\mu} = \frac{\tilde{\delta}(1-2\tilde{K}e^{-\tilde{\gamma}\tilde{\tau}})}{2e^{-\tilde{\gamma}\tilde{\tau}}-1}$. If the conditions,

$$\begin{cases} 0 < \tilde{\alpha} < 1, \quad \mu < \beta(0), \quad \tilde{\mu} < \tilde{\beta}(0), \\ \tilde{\alpha}\beta^{-1}(\mu) < \tilde{\beta}^{-1}(\tilde{\mu}) < \beta^{-1}(\mu), \\ 2\tilde{K}e^{-\tilde{\gamma}\tilde{\tau}} < 1 < 2e^{-\tilde{\gamma}\tilde{\tau}}, \end{cases} \tag{25}$$

or,

$$\begin{cases} \tilde{\alpha} > 1, \quad \mu < \beta(0), \quad \tilde{\mu} < \tilde{\beta}(0), \\ \beta^{-1}(\mu) < \tilde{\beta}^{-1}(\tilde{\mu}) < \tilde{\alpha}\beta^{-1}(\mu), \\ 2\tilde{K}e^{-\tilde{\gamma}\tilde{\tau}} < 1 < 2e^{-\tilde{\gamma}\tilde{\tau}}, \end{cases} \tag{26}$$

are satisfied, then a unique strictly positive dormancy steady state $\mathfrak{D} = (\tilde{x}_e, \tilde{u}_e, x_e)$, exists and is given by (17).

Remark 2. (1) Obviously, uniqueness in Proposition 1(vii) means the existence of a unique isolated strictly positive equilibrium point $\mathfrak{D}$, but the trivial steady state and the points $\mathfrak{E} = (0, 0, x_e)$, $(\tilde{x}_e, \tilde{u}_e, 0)$ are also steady states of system (10). (2) We can check that when the positive steady states exists, then

$$y_e = \frac{1}{\gamma}(1 - e^{-\gamma\tau})\beta(x_e + \tilde{x}_e)x_e, \quad \text{and,} \quad \tilde{y}_e = \frac{1}{\tilde{\gamma}}(1 - e^{-\tilde{\gamma}\tilde{\tau}})\tilde{u}_e, \tag{27}$$

where y_e (resp. $\tilde{y}_e$) is the positive steady state of the total density of proliferating healthy (resp. unhealthy) cells. (3) The third condition in (25) and (26) expresses an interesting relationship between the fast-self renewing ability $\tilde{K}$, the apoptosis rate of malignant cancer cells $\tilde{\gamma}$, and their average cell-cycle duration $\tilde{\tau}$. We notice that even if $\tilde{K}$ is relatively important (and knowing that it is not easy to act on $\tilde{K}$ by drug infusions since its high value is due to FLT3 mutations) it is still possible to guarantee the existence of a dormancy state by increasing $\tilde{\tau}\tilde{\gamma}$. However, the increase must be moderate to not exceed the upper-bound $\tilde{\gamma}\tilde{\tau} < \ln(2)$. (4) Finally, we notice that other cases can be discussed if biologically needed. For instance, adding the restriction, $2\tilde{\beta}^{-1}(\tilde{\mu}) < (1 + \tilde{\alpha})\beta^{-1}(\mu)$, to the conditions (25) and (26), ensures that $x_e > \tilde{x}_e$, which can reasonably be the expected situation of dormant tumors without forming clinically apparent cancers.

Now, we motivate our stability analysis through some preliminary numerical observations that highlight the rich dynamics of the model that we introduced in this work. In particular, we point out the different possible behaviors of the nonlinear differential-difference system (10) according to its associated initial conditions. The latter fact emphasizes the importance of determining mathematically an estimate of the region of attraction of each steady state of interest.

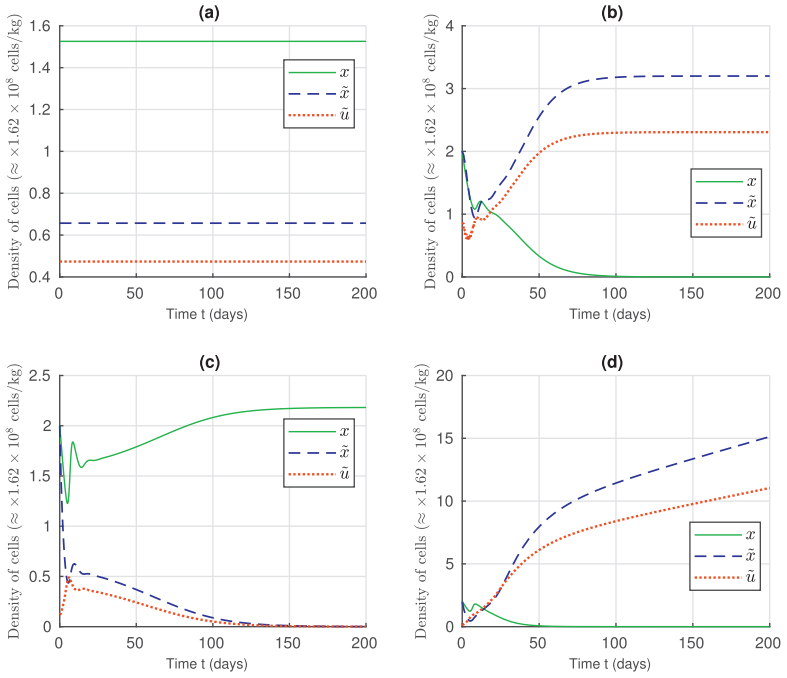

Fig. 4. (a) Trajectories of the model whose parameters are given in Example 1, when they started on the Dormancy steady state $\mathfrak{D}$, where $\tilde{x}_e = 0.6573$, $\tilde{u}_e = 0.4737$ and $x_e = 1.5255$. We mention that in this case, numerical simulations show that $\mathfrak{D}$ is unstable, i.e. for arbitrary small perturbation on the initial conditions, trajectories do not converge towards $\mathfrak{D}$. (b) Trajectories of the model whose parameters are given in Example 1, when they started from the initial conditions given by: $\varphi_x(t) = \varphi_{\tilde{x}}(t) = 2$, for all $t \in [-\tau, 0]$, and $\varphi_{\tilde{u}}(t) = 1$, for all $t \in [-\tilde{\tau}, 0]$. The steady states $\mathfrak{D}$ and $\mathfrak{E}$ both exist in this case, however, we notice that the trajectories rather converge to another equilibrium point, that seems stable, and which is given by (3.1998, 2.3060, 0). (c) All the model parameters and the initial conditions are similar to (b), except the initial condition for $\tilde{u}$ which is no given by: $\varphi_{\tilde{u}}(t) = 0.1$, for all $t \in [-\tilde{\tau}, 0]$. In this case, the trajectories converge to $\mathfrak{E} = (0, 0, 2.1826)$. (d) Now, we modify the value of $\tilde{K}$, that we increase to 0.6680, and we observe that for any initial conditions the trajectories $\tilde{x} \to +\infty$ and $\tilde{u} \to +\infty$, when t goes to $+\infty$.

Example 1. Let us consider the following biological functions and parameters for cells in Category A (Cat. A) and Category B (Cat. B):

Cat. A:	$\tau = 1.11$	$\delta = 0.1$	$\gamma = 0.1$	$\beta(m) = \frac{3}{1+m^4}$		
Cat. B:	$\tilde{\tau} = 0.9$	$\tilde{\delta} = 0.36$	$\tilde{\gamma} = 0.32$	$\tilde{\beta}(m) = \frac{2}{1+m^4}$	$\tilde{\alpha} = 0.6$	$\tilde{K} = 0.54$

For the considered set of parameters and functions, a unique dormancy steady state $\mathfrak{D}$ exists and is given by $\mathfrak{D} = (\tilde{x}_e, \tilde{u}_e, x_e)$, where $\tilde{x}_e = 0.6573$, $\tilde{u}_e = 0.4737$ and $x_e = 1.5255$. This steady state is shown in Fig. 4(a). However, the latter point is not the unique equilibrium point of the system. Indeed, the 0-equilibrium (0, 0, 0), and the points: $\mathfrak{E} = (0, 0, 2.1826)$ and (3.1998, 2.3060, 0), also exist.[8] When we select the constant initial conditions $\varphi_x(t) = \varphi_{\tilde{x}}(t) = 2$, for all $t \in [-\tau, 0]$, and $\varphi_{\tilde{u}}(t) = 1$, for all $t \in [-\tilde{\tau}, 0]$, we observe that the trajectories converge to (3.1998, 2.3060, 0), as illustrated in Fig. 4(b), where unhealthy cells survive (the attractive point seems to be stable), while the healthy cells vanish (converge to zero). By changing the initial condition of $\tilde{u}$, from the previous value to $\varphi_{\tilde{u}}(t) = 0.1$, for all $t \in [-\tilde{\tau}, 0]$, we observe that the trajectories converge to $\mathfrak{E}$, as illustrated in Fig. 4(c). Moreover, the steady states in Fig. 4(b) and (c) seem to be stable (each one has its region of attraction). Lyapunov theory offers strong tools to establish the regional stability properties of the steady states, provided that a suitable Lyapunov functional is found for the studied model. Now, let us modify the value of $\tilde{K}$ by increasing it to $\tilde{K} = 0.6680$. It follows that $2\tilde{K}e^{-\tilde{\gamma}\tilde{\tau}} - 1 = 0.017$, which implies that the trajectories of the unhealthy compartment are unbounded (similarly to Adimy et al., 2015). Numerical simulations in that case, for arbitrary initial conditions, are given in Fig. 4(d).

Example 2. Now, let us consider the following functions and parameters:

Cat. A:	$\tau = 1.25$	$\delta = 0.2$	$\gamma = 0.2$	$\beta(m) = \frac{1}{1+m^2}$		
Cat. B:	$\tilde{\tau} = 1.66$	$\tilde{\delta} = 0.1$	$\tilde{\gamma} = 0.2$	$\tilde{\beta}(m) = \frac{1.2}{1+5m^4}$	$\tilde{\alpha} = 0.4$	$\tilde{K} = 0.3$

The steady states (0, 0, 0), $\mathfrak{E} = (0, 0, x_e)$, $(\tilde{x}_e, \tilde{u}_e, 0)$, and $\mathfrak{D} = (\tilde{x}_e, \tilde{u}_e, x_e)$, of the corresponding system, exist. If we select the constant initial conditions $\varphi_x(t) = 1.55$, and $\varphi_{\tilde{x}}(t) = 1$, for all $t \in [-\tau, 0]$, and $\varphi_{\tilde{u}}(t) = 0.3$, for all $t \in [-\tilde{\tau}, 0]$, we observe that the trajectories are unstable as illustrated in Fig. 5(a), knowing that the dormancy steady state here is $\mathfrak{D} = (0.3445, 0.0792, 0.9926)$. For instance, we recall that in hematopoietic systems, oscillations are associated to many periodic diseases (e.g. cyclic neutropenia and some types of chronic leukemia). Now, let us consider random constant initial conditions and let us keep constant all the biological parameters, except the value of $\tilde{\alpha}$, that we consider as 0.2, and then 0.6 in a second case. As shown in Fig. 5(b), we note that by increasing the value of $\tilde{\alpha}$ from 0.2 to 0.6, the trajectories become stable. Thus, it appears that $\tilde{\alpha}$ may have, at least in this example, a stabilizing (or destabilizing) effect on the trajectories of the studied model.

Example 3. Finally, let us consider the following functions and parameters:

Cat. A:	$\tau = 1.25$	$\delta = 0.1$	$\gamma = 0.2$	$\beta(m) = \frac{1}{1+m^2}$		
Cat. B:	$\tilde{\tau} = 0.7$	$\tilde{\delta} = 0.2$	$\tilde{\gamma} = 0.1$	$\tilde{\beta}(m) = \frac{2}{1+2m^4}$	$\tilde{\alpha} = 2$	$\tilde{K} = 0.5$

The conditions of existence of $\mathfrak{D} = (\tilde{x}_e, \tilde{u}_e, x_e)$ are satisfied, and in this case we have: $\tilde{x}_e = 0.6833$, $\tilde{u}_e = 0.1580$ and $x_e = 1.45599$. For the constant initial conditions $\varphi_x(t) = 0.1$ and $\varphi_{\tilde{x}}(t) = 1.5$, for

[8] One may notice the relationship that exists between the three different non-trivial steady states. In fact, the x_e-value in $\mathfrak{E}$ corresponds to the sum $x_e + \tilde{x}_e$ of the dormancy steady state $\mathfrak{D}$, while the $\tilde{x}_e$-value in the steady state $(\tilde{x}_e, \tilde{u}_e, 0)$ corresponds to the value $\frac{x_e + \tilde{\alpha}\tilde{x}_e}{\tilde{\alpha}}$, where x_e and $\tilde{x}_e$ in the latter fraction are the corresponding values in the dormancy steady state $\mathfrak{D}$.

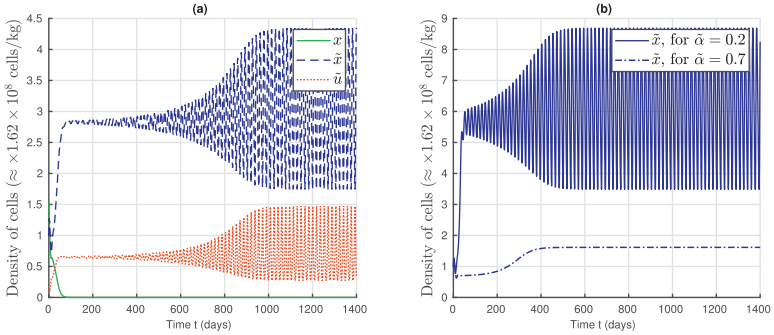

Fig. 5. Trajectories of the model in Example 2. (a) Unstable (oscillatory) solutions corresponding to the constant initial conditions $\varphi_x(t) = 1.55$, $\varphi_{\tilde{x}}(t) = 1$, for all $t \in [-\tau, 0]$, $\varphi_{\tilde{u}}(t) = 0.3$, for all $t \in [-\tilde{\tau}, 0]$. (b) Stabilizing effect of $\tilde{\alpha}$. In this illustration, all the parameters, as well as initial conditions, are identical, except the value of $\tilde{\alpha}$. In the first case, $\tilde{\alpha} = 0.2$: the trajectories are unstable. By increasing $\tilde{\alpha}$ to 0.7 the trajectories become stable.

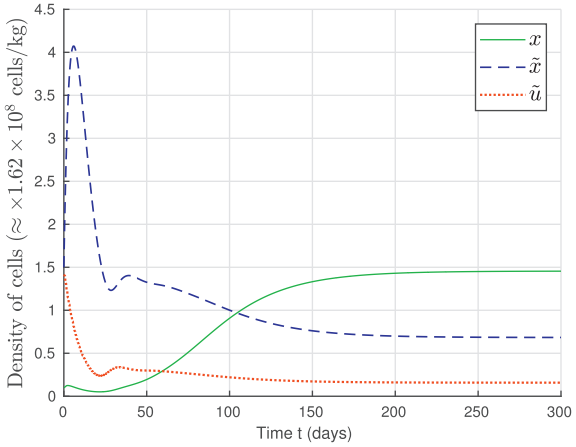

Fig. 6. Trajectories of the model given in Example 3. Here the dormancy steady state $\mathfrak{D}$ exists and is given by: $\tilde{x}_e = 0.6833$, $\tilde{u}_e = 0.1580$ and $x_e = 1.45599$. Convergence to the dormancy steady state $\mathfrak{D}$ (which seems stable) is obtained starting from the constant initial conditions: $\varphi_x(t) = 0.1$ and $\varphi_{\tilde{x}}(t) = 1.5$, for all $t \in [-\tau, 0]$, and $\varphi_{\tilde{u}}(t) = 1.5$ for all $t \in [-\tilde{\tau}, 0]$.

all $t \in [-\tau, 0]$, and $\varphi_{\tilde{u}}(t) = 1.5$ for all $t \in [-\tilde{\tau}, 0]$, it appears that $\mathfrak{D}$ is stable as illustrated in Fig. 6.

At this juncture, we deduce that the coupled system (10) under study has some interesting dynamical features. Firstly, we saw that the solutions of the coupled system can be bounded or unbounded (as in the non-coupled model, Adimy et al., 2015). In the former case, several steady states may exist and their values depend on the different biological parameters of the model. The existence of the steady states of interest ($\mathfrak{D}$ and $\mathfrak{E}$) are governed by some non-intuitive conditions on the biological parameters involved in the system (see Proposition 1). In addition, we saw that according to the initial conditions associated with the model trajectories, the bounded solutions may converge to one among several possible steady states, i.e. the stability of each steady state is regional (local). In the general case, the steady states of the system (10) are not always stable, but on the contrary, we noticed that oscillations may emerge, as in Example 2. Our objective now is to determine exponential stability conditions for the steady states of interest (which are: all-cell extinction, $\mathfrak{E}$ and $\mathfrak{D}$).

4. Stability analysis of the extinction of all the cells

In this section, we perform a stability analysis of the 0-equilibrium of the system (10). From a biological standpoint, this is a case that we want to avoid, as discussed in the previous section (see the first point, *Cell extinction*), since it is synonymous of an excessive therapy that not only alters unhealthy populations, but also leads to the extinction of healthy cells in the coupled model.

Here we introduce the following functional:

$$\begin{aligned}\mathcal{W}(\tilde{x}_t, \tilde{u}_t, x_t) =& \tilde{x}(t) + x(t) + \psi_1 \int_{t-\tilde{\tau}}^{t} e^{\rho_1^*(\ell - t)} \tilde{u}(\ell) d\ell \\ &+ \psi_2 \int_{t-\tau}^{t} e^{\rho_2^*(\ell - t)} \beta(x(\ell) + \tilde{x}(\ell)) x(\ell) d\ell,\end{aligned} \tag{28}$$

where, $\psi_1 = \psi_{11} + \psi_{12}$, $\psi_{11} = 1 + \frac{\tilde{\delta}}{\tilde{\beta}(0)}$, $\psi_{12} = -\frac{\psi^*}{3(\overline{K} - \tilde{K})\tilde{\beta}(0)}$, $\overline{K} = \frac{1}{2} e^{\tilde{\gamma}\tilde{\tau}}$, $\psi^* = (\tilde{\beta}(0) + \tilde{\delta})\overline{K} - \tilde{\beta}(0) - \tilde{K}\tilde{\delta}$, and, $\psi_2 = 2\psi_3 e^{-\gamma\tau}$, where, ψ_3, together with ρ_1^* and ρ_2^*, are strictly positive constants that we will choose later.

We can readily check that if $2\tilde{K}e^{-\tilde{\gamma}\tilde{\tau}} < 1$ (that we can rewrite as $\tilde{K} < \overline{K}$), and $\psi^* > 0$, (i.e. $\psi_{12} < 0$), we obtain $\psi_1 > 0$. It follows that the functional $\mathcal{W}$ is nonnegative. We notice also that $\mathcal{W}$ is an unusual Lyapunov–Krasovskii functional (LKF) candidate, since it can be used only because the system (10) is positive. In addition, it is a *degenerate* LKF candidate (since $\mathcal{W} = 0$ does not imply $\tilde{u} = 0$) which is usually the case for differential-difference systems. This will also be the case when we investigate the stability properties of the dormancy steady state, where we will construct a quadratic degenerate LKF.

Thanks to the functional $\mathcal{W}$, we prove in Appendix A the following result:

Theorem 1. *If the conditions*

$$\left(2e^{-\gamma\tau} - 1\right)\beta(0) < \delta, \quad 0 < \psi^*, \quad \text{and,} \quad 2\tilde{K}e^{-\tilde{\gamma}\tilde{\tau}} < 1, \tag{29}$$

are satisfied, then the trivial steady state of system (10) is globally exponentially stable with a decay rate larger than, or equal to, ψ_4 (defined in Appendix A).

Remark 3. (1) The conditions (29) exclude the existence of any steady state different from the trivial one. (2) We can interpret the cell extinction as a result of an excessive therapy that affects also healthy cells so that their apoptosis rate, γ, increases until becoming greater than the ratio $\frac{\ln(2)}{\tau}$, or, until the death rate and differentiation rate, i.e. δ, becomes greater than $(2e^{-\gamma\tau} - 1)\beta(0)$ (which is a less demanding condition in comparison to $\gamma > \frac{\ln(2)}{\tau}$). (3) Arguing as in Adimy et al. (2015), Djema et al. (2016a), we can prove that the conditions (29) are also necessary for the exponential stability of the 0-equilibrium. (4) Finally, we deduce from Theorem 1 that all-cell extension results from uncorrelated conditions between the healthy and unhealthy compartments. Indeed, we note that the last two conditions in (29) relate to the unhealthy compartment, since only unhealthy parameters are involved. Moreover, these conditions are similar to those giving global asymptotic stability in Adimy et al. (2015) for a non-coupled model. The biological interpretation is that cell extension occurs if and only if

both the healthy and unhealthy compartments are enable to regenerate themselves autonomously. In other words, it appears that the coupling has no effect on the stability of the 0-equilibrium since the conditions for total-cell eradication imply extinction of both the unhealthy and healthy compartments, as if they were separated (not coupled). This observation will not hold when we study dormancy (and non-zero steady states).

5. Stability analysis of favorable steady states: $\mathfrak{D}$ (dormancy) and $\mathfrak{E}$ (CSCs eradication)

Here we will emphasize on the dormancy steady state $\mathfrak{D} = (\tilde{x}_e, \tilde{u}_e, x_e)$, where all the components of the steady state are different from zero (i.e. $\tilde{x}_e > 0,\ \tilde{u}_e > 0,\ x_e > 0$). In fact, we will highlight the case of dormancy $\mathfrak{D}$, since it is clearly the most general one. Indeed, from the analysis of $\mathfrak{D}$, it becomes possible to evaluate the regional stability properties of $\mathfrak{E} = (0, 0, x_e)$ (which are partially investigated in Djema et al., 2016b, when $\tilde{\alpha} = 1$), and also of the steady state $(\tilde{x}_e, \tilde{u}_e, 0)$.

5.1. A new representation of the system

Now, we want to investigate the stability properties of $\mathfrak{D}$ when it exists. Thus, we assume that the conditions given in *Proposition 1*(vii) are satisfied and we perform the classical changes of coordinates: $\tilde{X} = \tilde{x} - \tilde{x}_e$, $\tilde{U} = \tilde{u} - \tilde{u}_e$, and $X = x - x_e$. Therefore, from (10), it follows that for all $t \geq 0$,

$$\begin{cases} \dot{\tilde{X}}(t) = -\big[\tilde{\delta} + \tilde{\beta}(X(t) + \tilde{\alpha}\tilde{X}(t) + x_e + \tilde{\alpha}\tilde{x}_e)\big](\tilde{X}(t) + \tilde{x}_e) \\ \qquad\qquad +2(1-\tilde{K})e^{-\tilde{\gamma}\tilde{\tau}}(\tilde{U}(t-\tilde{\tau}) + \tilde{u}_e), \\ \tilde{U}(t) + \tilde{u}_e = \tilde{\beta}(X(t) + \tilde{\alpha}\tilde{X}(t) + x_e + \tilde{\alpha}\tilde{x}_e)(\tilde{X}(t) + \tilde{x}_e) \\ \qquad\qquad +2\tilde{K}e^{-\tilde{\gamma}\tilde{\tau}}(\tilde{U}(t-\tilde{\tau}) + \tilde{u}_e), \\ \dot{X}(t) = -\big[\delta + \beta(X(t) + \tilde{X}(t) + x_e + \tilde{x}_e)\big](X(t) + x_e) \\ \qquad\qquad +2e^{-\gamma\tau}\beta(X(t-\tau) + \tilde{X}(t-\tau) + x_e + \tilde{x}_e)(X(t-\tau) + x_e). \end{cases} \tag{30}$$

To ease the analysis of the above system, we rewrite it in a more convenient form. Observe that for all $\mathfrak{z} > -\mathfrak{e},\ \mathfrak{e} > 0$, where, $\mathfrak{z} = X + \tilde{X}$ and $\mathfrak{e} = x_e + \tilde{x}_e$, we have, with an abuse of notation,

$$\beta(\mathfrak{z} + \mathfrak{e}) = \beta(\mathfrak{e}) + \theta\mathfrak{z} + R(\mathfrak{z}), \tag{31}$$

where β is the Hill-function defined in (1), $\theta = \beta'(\mathfrak{e})$, and, $R(\mathfrak{z}) = \int_{\mathfrak{e}}^{\mathfrak{e}+\mathfrak{z}} (\mathfrak{z} + \mathfrak{e} - \ell)\beta^{(2)}(\ell)d\ell$. Next, for all $\tilde{\mathfrak{z}} > -\tilde{\mathfrak{e}},\ \tilde{\mathfrak{e}} > 0$, where, $\tilde{\mathfrak{z}} = X + \tilde{\alpha}\tilde{X}$, and, $\tilde{\mathfrak{e}} = x_e + \tilde{\alpha}\tilde{x}_e$, we get similarly to (31),

$$\tilde{\beta}(\tilde{\mathfrak{z}} + \tilde{\mathfrak{e}}) = \tilde{\beta}(\tilde{\mathfrak{e}}) + \tilde{\theta}\tilde{\mathfrak{z}} + \tilde{R}(\tilde{\mathfrak{z}}), \tag{32}$$

where, $\tilde{\theta} = \tilde{\beta}'(\tilde{\mathfrak{e}})$, and, $\tilde{R}(\tilde{\mathfrak{z}}) = \int_{\tilde{\mathfrak{e}}}^{\tilde{\mathfrak{e}}+\tilde{\mathfrak{z}}} (\tilde{\mathfrak{z}} + \tilde{\mathfrak{e}} - \ell)\tilde{\beta}^{(2)}(\ell)d\ell$. Therefore, using (31) and (32), and by simplifying some terms using (11), we get the system,

$$\begin{cases} \dot{\tilde{X}}(t) = -\mathfrak{a}_1\tilde{X}(t) - \mathfrak{a}_2X(t) + \mathfrak{a}_3\tilde{U}(t-\tilde{\tau}) + F(X(t), \tilde{X}(t)), \\ \tilde{U}(t) = \mathfrak{a}_4\tilde{X}(t) + \mathfrak{a}_2X(t) + \mathfrak{a}_5\tilde{U}(t-\tilde{\tau}) - F(X(t), \tilde{X}(t)), \\ \dot{X}(t) = -\mathfrak{a}_6X(t) - \mathfrak{a}_7\tilde{X}(t) + \mathfrak{a}_8X(t-\tau) + \mathfrak{a}_9\tilde{X}(t-\tau) + G(X_t, \tilde{X}_t), \end{cases} \tag{33}$$

$$\begin{aligned} \text{where,} \qquad F(X(t), \tilde{X}(t)) = &-\tilde{\theta}\big[\tilde{\alpha}\tilde{X}^2(t)) + X(t)\tilde{X}(t)\big] \\ &- \tilde{R}(X(t) + \tilde{\alpha}\tilde{X}(t))(\tilde{X}(t) + \tilde{x}_e), \end{aligned} \tag{34}$$

$$\begin{aligned} G(X_t, \tilde{X}_t) = &-\theta\big[X^2(t) + X(t)\tilde{X}(t)\big] - R(X(t) + \tilde{X}(t))(X(t) + x_e) \\ &+ 2e^{-\gamma\tau}\theta\big[X^2(t-\tau) + X(t-\tau)\tilde{X}(t-\tau)\big] \\ &+ 2e^{-\gamma\tau}R(X(t-\tau) + \tilde{X}(t-\tau))(X(t-\tau) + x_e), \end{aligned} \tag{35}$$

and where the constant parameters $\mathfrak{a}_i$ are given by:

$$\begin{cases} \mathfrak{a}_1 = \tilde{\delta} + \tilde{\beta}(x_e + \tilde{\alpha}\tilde{x}_e) + \tilde{\alpha}\tilde{\theta}\tilde{x}_e, \quad \mathfrak{a}_2 = \tilde{\theta}\tilde{x}_e, \quad \mathfrak{a}_3 = 2(1-\tilde{K})e^{-\tilde{\gamma}\tilde{\tau}}, \\ \mathfrak{a}_4 = \tilde{\beta}(x_e + \tilde{\alpha}\tilde{x}_e) + \tilde{\alpha}\tilde{\theta}\tilde{x}_e, \ \mathfrak{a}_5 = 2\tilde{K}e^{-\tilde{\gamma}\tilde{\tau}}, \ \mathfrak{a}_6 = \delta + \beta(x_e + \tilde{x}_e) + \theta x_e, \\ \mathfrak{a}_7 = \theta x_e, \quad \mathfrak{a}_8 = 2e^{-\gamma\tau}[\beta(x_e + \tilde{x}_e) + \theta x_e], \quad \mathfrak{a}_9 = 2e^{-\gamma\tau}\theta x_e. \end{cases} \tag{36}$$

We notice that if the trajectories of (33) converge exponentially to the 0-equilibrium, then the positive trajectories of the system (10) converge exponentially to $\mathfrak{D}$. Now, we are going to state and prove some sector conditions on the nonlinear terms R and $\tilde{R}$. Then, we deduce some upper-bounds on the nonlinear terms F and G. For that purpose, we prove in Appendix B through lengthy calculations that there exist strictly positive constants $\mathfrak{s}$, $\tilde{\mathfrak{s}}$, $\mathfrak{m}$ and $\tilde{\mathfrak{m}}$, satisfying:

$$|R(\mathfrak{z})| \leq \mathfrak{s}|\mathfrak{z}|, \quad \text{and} \quad |\tilde{R}(\tilde{\mathfrak{z}})| \leq \tilde{\mathfrak{s}}|\tilde{\mathfrak{z}}|, \tag{37}$$

$$|R(\mathfrak{z})| \leq \mathfrak{m}\mathfrak{z}^2, \quad \text{and} \quad |\tilde{R}(\tilde{\mathfrak{z}})| \leq \tilde{\mathfrak{m}}\tilde{\mathfrak{z}}^2, \tag{38}$$

for all $\mathfrak{z} > -\mathfrak{e}$ ($\mathfrak{z}$ and $\mathfrak{e}$ are defined before (31)), and for all $\tilde{\mathfrak{z}} > -\tilde{\mathfrak{e}}$ ($\tilde{\mathfrak{z}}$ and $\tilde{\mathfrak{e}}$ are defined before (32)). Moreover, using (37) and (38), we can determine strictly positive constants $\mathfrak{c}_i,\ i = \{1, \ldots, 6\}$, such that the following quadratic upper bounds hold true:

$$\big|F(X, \tilde{X})\big| \leq \mathfrak{c}_1Q(X) + \mathfrak{c}_2Q(\tilde{X}), \tag{39}$$

$$\begin{aligned} \big|G(X_t, \tilde{X}_t)\big| \leq\ &\mathfrak{c}_3Q(X(t)) + \mathfrak{c}_4Q(\tilde{X}(t)) + \mathfrak{c}_5Q(X(t-\tau)) \\ &+ \mathfrak{c}_6Q(\tilde{X}(t-\tau)). \end{aligned} \tag{40}$$

Remark 4. (1) The upper-bounds given in (37)–(40), will not intervene when we determine the decay conditions and the decay rate of the solutions. However, their effect appears in the size of the basin of attraction that we will provide. Actually, if the constants $\mathfrak{s}$, $\tilde{\mathfrak{s}}$, $\mathfrak{m}$, $\tilde{\mathfrak{m}}$, in (37) and (38), as well as the constants $\mathfrak{c}_i$ in (39) and (40), are large, then the size of the basin of attraction shrinks accordingly. (2) By comparing the present study with Djema et al. (2016b), we notice that Djema et al. (2016b) was devoted to the study of a model which was simpler than the system (33) under study in this paper. Indeed, the model in Djema et al. (2016b) can be obtained by putting $\tilde{\alpha} = 1$ and by eliminating all the terms where $\tilde{x}_e$ is present in Eqs. (33)–(36). (3) It is worth mentioning that the stability results that we will determine later apply for a wide range of functions β and $\tilde{\beta}$, as long as the sector conditions (37) and (38) are satisfied.

Now, we want to perform a stability analysis of the trivial steady state of the (shifted) model using its representation in (33): we recall that the 0-equilibrium of (33) can be $\mathfrak{D}$ or $\mathfrak{E}$ of (10). For meeting such a purpose, strong tools are provided by Lyapunov theory, in the analysis of nonlinear differential-difference systems with possibly piecewise continuous solutions (see e.g. Gu and Liu, 2009; Karafyllis et al., 2009; Michel et al., 2015; Pepe, 2003, and the references therein). However, finding a suitable LKF is not an easy task. In addition, the provided stability conditions can be conservative. So, we adopt the following strategy that highlights our biological aims:

① Firstly, we use the *descriptor method* (Fridman, 2014) that allows us to provide a local (Lyapunov-based) stability result for our biological model. The advantage of this approach is that it provides an effective tool (formulated as an LMI condition) to check if a steady state of a specific biological model (defined by its set of parameters) is locally stable.

② In order to address the following issue: *How can we provide realistic stability conditions that can be interpreted and satisfied under the effect of drugs?* The first approach will be slightly modified

in a second time. Thus, we establish a different result (that can be seen as a particular formulation of the first approach) which relies on the analytic construction of a suitable Lyapunov-like functional, specific for the studied biological system. The latter approach allows us to provide more explicit decay conditions than the common LMI-type approaches. We point out that even if the second construction provides more conservative conditions than the LMI ones, they have the advantage of being more easily (biologically) understandable. It is to this end that, in the last section, we show how the decay conditions can be interpreted, in practice, according to the biological context of hematopoiesis and leukemia.

In summary, we determine throughout this section some exponential decay conditions (along with an estimate of the decay rate of the solutions and a region of attraction of the favorable steady states), via two complementary approaches: the descriptor method that provides local stability results for the general structure of the studied system, and, a suitable explicit Lyapunov-like construction that allows us to address the regional stability properties of the dormancy steady state. The latter decay conditions lend themselves more easily than the LMI ones to medical interpretations.

5.2. Stability analysis using the descriptor method

In this section, we consider as a first step only continuous solutions of the system in (33) and we study the linear approximation of the state $col\{X, \tilde{X}\}$, that we denote $Z = col\{Z_1, Z_2\}$. Then, by neglecting the nonlinear terms F and G in (33), we rewrite the studied system in the following compact form:

$$\begin{cases} \dot{Z}(t) = B_0 Z(t) + B_1 Z(t-\tau) + B_2 \tilde{U}(t-\tilde{\tau}), \\ \tilde{U}(t) = B_3 Z(t) + B_4 \tilde{U}(t-\tilde{\tau}), \end{cases} \tag{41}$$

for all $t \geq 0$, where B_i are given by (we recall that $\mathfrak{a}_i$ are defined in (36)),

$$B_0 = -\begin{pmatrix} \mathfrak{a}_6 & \mathfrak{a}_7 \\ \mathfrak{a}_2 & \mathfrak{a}_1 \end{pmatrix}, \quad B_1 = \begin{pmatrix} \mathfrak{a}_8 & \mathfrak{a}_9 \\ 0 & 0 \end{pmatrix}, B_2 = \begin{pmatrix} 0 \\ \mathfrak{a}_3 \end{pmatrix}, \\ B_3 = \begin{pmatrix} \mathfrak{a}_2 & \mathfrak{a}_4 \end{pmatrix}, \text{ and, } B_4 = \mathfrak{a}_5 = 2\tilde{K} e^{-\tilde{\gamma}\tilde{\tau}}. \tag{42}$$

Next, we consider some symmetric positive definite matrices $P > 0$, $S > 0$, $J > 0$, of appropriate dimension, together with a strictly positive constant $\tilde{\mathfrak{a}}$, and we verify that the derivative of the functional,

$$V(Z_t, \tilde{U}_t) = Z(t)^T P Z(t) + \int_{t-\tau}^{t} Z^T(\ell) S Z(\ell) d\ell + \\ + \tilde{\mathfrak{a}} \int_{t-\tilde{\tau}}^{t} \tilde{U}^2(\ell) d\ell + \tau \int_{t-\tau}^{t} (\ell + \tau - t) \dot{Z}^T(\ell) J \dot{Z}(\ell) d\ell, \tag{43}$$

along the trajectories of (41), is given by,

$$\dot{V}(t) = Z^T(t)\left[P + P^T\right]\dot{Z}(t) + Z^T(t) S Z(t) - Z^T(t-\tau) S Z(t-\tau) \\ -\tau \int_{t-\tau}^{t} \dot{Z}^T(\ell) J \dot{Z}(\ell) d\ell + \tau^2 \dot{Z}^T(t) J \dot{Z}(t) + \tilde{\mathfrak{a}}\left(\tilde{U}^2(t) - \tilde{U}^2(t-\tilde{\tau})\right).$$

First, we notice that an upper-bound of $\dot{V}$ is given by,

$$\dot{V}(t) \leq Z^T(t)\left[P + P^T\right]\dot{Z}(t) + Z^T(t) S Z(t) - Z^T(t-\tau) S Z(t-\tau) \\ +\tau^2 \dot{Z}^T(t) J \dot{Z}(t) - Z^T(t) J Z(t) + Z^T(t) J Z(t-\tau) \\ +Z^T(t-\tau) J Z(t) - Z^T(t-\tau) J Z(t-\tau) + \tilde{\mathfrak{a}} \tilde{U}^2(t) - \tilde{\mathfrak{a}} \tilde{U}^2(t-\tilde{\tau}) \\ +2\left[Z^T(t)\overline{P}^T + \dot{Z}^T(t)\overline{\overline{P}}^T\right] \\ \underbrace{\left[B_0 Z(t) + B_1 Z(t-\tau) + B_2 \tilde{U}(t-\tilde{\tau}) - \dot{Z}(t)\right]}_{=0}, \tag{44}$$

which, in fact, directly follows from Jensen's Inequality given by,

$$-\tau \int_{t-\tau}^{t} \dot{Z}^T(\ell) J \dot{Z}(\ell) d\ell \leq -\int_{t-\tau}^{t} \dot{Z}^T(\ell) d\ell J \int_{t-\tau}^{t} \dot{Z}(\ell) d\ell \\ = -[Z(t) - Z(t-\tau)]^T J [Z(t) - Z(t-\tau)],$$

and where $\overline{P}$ and $\overline{\overline{P}}$ that appear in (44) are some free-weighting matrices of appropriate dimension. Then, it follows that,

$$\dot{V}(t) \leq \eta^T(t) \Phi \eta(t) + \tilde{\mathfrak{a}} \tilde{U}^2(t),$$

where η is an augmented state defined by,

$$\eta^T(t) = \begin{bmatrix} Z(t) & \dot{Z}(t) & Z(t-\tau) & \tilde{U}(t-\tilde{\tau}) \end{bmatrix}, \tag{45}$$

and the matrix Φ is given by,

$$\Phi = \begin{pmatrix} S - J + \overline{P}^T B_0 + B_0^T \overline{P} & P - \overline{P}^T + B_0^T \overline{\overline{P}} & J + \overline{P}^T B_1 & \overline{P}^T B_2 \\ * & \tau^2 J - \overline{\overline{P}}^T - \overline{\overline{P}} & \overline{\overline{P}}^T B_1 & \overline{\overline{P}}^T B_2 \\ * & * & -S - J & 0 \\ * & * & * & -\tilde{\mathfrak{a}} \end{pmatrix}. \tag{46}$$

Noticing that, $\tilde{U}(t) = [B_3 \quad 0 \quad 0 \quad B_4]\eta(t)$, it follows that,

$$\tilde{\mathfrak{a}} \tilde{U}^2(t) = \eta^T(t) E \eta(t), \quad \text{where, } E = \begin{bmatrix} B_3 & 0 & 0 & B_4 \end{bmatrix}^T \\ \tilde{\mathfrak{a}} \begin{bmatrix} B_3 & 0 & 0 & B_4 \end{bmatrix}.$$

Therefore, by applying Schur complement, we conclude that $\dot{V}(t) < 0$ is satisfied provided that the following LMI:

$$\Psi = \begin{pmatrix} S - J + \overline{P}^T B_0 + B_0^T \overline{P} & P - \overline{P}^T + B_0^T \overline{\overline{P}} & J + \overline{P}^T B_1 & \overline{P}^T B_2 & B_3^T \tilde{\mathfrak{a}} \\ * & \tau^2 J - \overline{\overline{P}}^T - \overline{\overline{P}} & \overline{\overline{P}}^T B_1 & \overline{\overline{P}}^T B_2 & 0 \\ * & * & -S - J & 0 & 0 \\ * & * & * & -\tilde{\mathfrak{a}} & B_4^T \tilde{\mathfrak{a}} \\ * & * & * & * & -\tilde{\mathfrak{a}} \end{pmatrix} \\ < 0, \tag{47}$$

holds. Next, by following arguments of Fridman (2002) we deduce from $\Psi < 0$ that the last block in (47) satisfies $\begin{pmatrix} -\tilde{\mathfrak{a}} & B_4^T \tilde{\mathfrak{a}} \\ * & -\tilde{\mathfrak{a}} \end{pmatrix} < 0$. The latter implies by Schur complement that $-I + B_4^T B_4 < 0$. Hence, the eigenvalues of B_4 are inside the unit circle, i.e. the difference equation $\tilde{U}(t) = B_4 \tilde{U}(t-\tilde{\tau})$ is stable for all $\tilde{\tau} > 0$. The latter, together with $\dot{V} < 0$, guarantees the asymptotic stability of the system (41). We mention that it is possible to extend the stability result to the nonlinear system (33), using the functional V (i.e. providing some conditions on the nonlinear terms F and G as in Fridman (2014, Section 3.11). However, since it seems actually difficult to interpret the LMI (47) as a combined targeted therapy for the studied biological system, we slightly modify our Lyapunov approach by designing, in the next section, a suitable specific LKF for the studied system that provides explicit (sufficient) stability conditions for the dormancy steady state of the nonlinear system (33). The functional that we are going to propose has some similarities with the functional V. Actually, in the next section, we are going to select some matrices P, S and J, together with the constant $\tilde{\mathfrak{a}}$, involved in the above construction. Thus, we will determine analytically some upper-bounds on $\dot{V}$, through classical inequalities. Not surprisingly, the latter approach increases the *conservatism* of the sufficient stability condition in the LMI form (the LMI condition is given by (47)). That is the price of determining more biologically exploitable results (i.e. explicit exponential decay conditions with an estimate on the decay rate of the solution and a subset of the basin of attraction of the trivial steady state of the nonlinear system (33)).

5.3. Obtaining explicit exponential decay conditions

We focus on the coupled system using its representation in (33), with possibly piecewise continuous solutions. Firstly, let us introduce the quadratic function:

$$\mathfrak{Q}(X,\tilde{X}) = Q(X) + \lambda_1 Q(\tilde{X}), \text{ where, } Q(\ell) = \tfrac{1}{2}\ell^2, \tag{48}$$

and $\lambda_1 = 2$. This is equivalent to put $P = diag\{1/2, 1\}$ in V of the previous section. Next, we consider the following operators,

$$\mathcal{Y}(\tilde{\varphi}) = \int_{-\tilde{\tau}}^{0} e^{\rho_1 \ell} Q(\tilde{\varphi}(\ell)) d\ell, \quad \text{and,} \tag{49}$$

$$\mathcal{S}(\varphi) = \int_{-\tau}^{0} e^{\rho_2 \ell} Q(\varphi(\ell)) d\ell, \tag{50}$$

where, $\varphi \in \mathcal{C}([-\tau, 0], \mathbb{R})$, $\tilde{\varphi} \in \mathcal{C}([-\tilde{\tau}, 0], \mathbb{R})$, and ρ_1, ρ_2, are strictly positive constants that we determine later. In fact, observe that, compared to the integral terms in V of the previous section, $\mathcal{S}$ and $\mathcal{Y}$ have exponential functions -in the integral terms- that make it possible to get a lower-bound on the exponential decay of the solutions. Next, in the quest for explicit decay conditions, we are going to substitute $\dot{X}$ and $\dot{\tilde{X}}$ when computing the derivative of $\mathfrak{Q}$ (which is not the approach adopted in the descriptor method, where $\dot{X}$ and $\dot{\tilde{X}}$ were not replaced). Thus, the derivative of $\mathfrak{Q}$ along the trajectories of (33), satisfies

$$\begin{aligned}\dot{\mathfrak{Q}}(t) =& -2\mathfrak{a}_1\lambda_1 Q(\tilde{X}(t)) - 2\mathfrak{a}_6 Q(X(t)) - (\mathfrak{a}_2\lambda_1 + \mathfrak{a}_7)X(t)\tilde{X}(t)\\ &+ \mathfrak{a}_3\lambda_1\tilde{X}(t)\tilde{U}(t-\tilde{\tau}) + \mathfrak{a}_8 X(t)X(t-\tau) + \mathfrak{a}_9 X(t)\tilde{X}(t-\tau)\\ &+ \lambda_1\tilde{X}(t)F(X(t),\tilde{X}(t)) + X(t)G(X_t,\tilde{X}_t).\end{aligned} \tag{51}$$

Notice that the derivative of $\mathcal{Y}(\tilde{U}_t)$, for almost all $t \geq 0$, is

$$\dot{\mathcal{Y}}(t) = Q(\tilde{U}(t)) - e^{-\rho_1\tilde{\tau}} Q(\tilde{U}(t-\tilde{\tau})) - \rho_1 \mathcal{Y}(\tilde{U}_t). \tag{52}$$

Now, using the second equation in (33), we obtain

$$\begin{aligned}\dot{\mathcal{Y}}(t) =& -\rho_1\mathcal{Y}(\tilde{U}_t) + \mathfrak{a}_4^2 Q(\tilde{X}(t)) + \mathfrak{a}_2^2 Q(X(t))\\ &- (e^{-\rho_1\tilde{\tau}} - \mathfrak{a}_5^2) Q(\tilde{U}(t-\tilde{\tau}))\\ &+ \mathfrak{a}_2\mathfrak{a}_4 X(t)\tilde{X}(t) + \mathfrak{a}_2\mathfrak{a}_5 X(t)\tilde{U}(t-\tilde{\tau}) + \mathfrak{a}_4\mathfrak{a}_5\tilde{X}(t)\tilde{U}(t-\tilde{\tau})\\ &+ Q(F(\tilde{X}(t),X(t))) - F(X(t),\tilde{X}(t))\\ &\Big[\mathfrak{a}_4\tilde{X}(t) + \mathfrak{a}_2 X(t) + \mathfrak{a}_5\tilde{U}(t-\tilde{\tau})\Big],\end{aligned}$$

where the $\mathfrak{a}_i$'s and F are defined after (33). Similarly, we compute the derivatives of the functionals $\mathcal{S}(X_t)$ and $\mathcal{S}(\tilde{X}_t)$. By combining the previous intermediate results (i.e. $\dot{\mathfrak{Q}}$, $\dot{\mathcal{Y}}$ and $\dot{\mathcal{S}}$), we deduce that the time derivative of the functional,

$$V^\dagger(X_t,\tilde{X}_t,\tilde{U}_t) = \mathfrak{Q}(X(t),\tilde{X}(t)) + \lambda_2\mathcal{S}(X_t) + \lambda_3\mathcal{S}(\tilde{X}_t) + \lambda_4\mathcal{Y}(\tilde{U}_t), \tag{53}$$

where λ_2, λ_3 and λ_4 are positive constants to be chosen later, along the trajectories of (33) is given, for almost all $t \geq 0$, by:

$$\begin{aligned}\dot{V}^\dagger(t) =& -\Big[2\lambda_1\mathfrak{a}_1 - \lambda_3 - \lambda_4\mathfrak{a}_4^2\Big]Q(\tilde{X}(t)) - \Big[2\mathfrak{a}_6 - \lambda_2 - \lambda_4\mathfrak{a}_2^2\Big]Q(X(t))\\ &- \rho_2\lambda_3\mathcal{S}(\tilde{X}_t) - \rho_2\lambda_2\mathcal{S}(X_t) - \rho_1\lambda_4\mathcal{Y}(\tilde{U}_t) - \lambda_4\Big[e^{-\rho_1\tilde{\tau}} - \mathfrak{a}_5^2\Big]Q(\tilde{U}(t-\tilde{\tau}))\\ &- \lambda_2 e^{-\rho_2\tau}Q(X(t-\tau)) - \lambda_3 e^{-\rho_2\tau}Q(\tilde{X}(t-\tau)) + \mathfrak{a}_2\mathfrak{a}_5\lambda_4 X(t)\tilde{U}(t-\tilde{\tau})\\ &- [\mathfrak{a}_2\lambda_1 + \mathfrak{a}_7 - \lambda_4\mathfrak{a}_2\mathfrak{a}_4]X(t)\tilde{X}(t) + \mathfrak{a}_8 X(t)X(t-\tau) + \mathfrak{a}_9 X(t)\tilde{X}(t-\tau)\\ &+ [\mathfrak{a}_3\lambda_1 + \mathfrak{a}_4\mathfrak{a}_5\lambda_4]\tilde{X}(t)\tilde{U}(t-\tilde{\tau}) - \mathfrak{a}_5\lambda_4 F(X(t),\tilde{X}(t))\tilde{U}(t-\tilde{\tau})\\ &+ X(t)G(X_t,\tilde{X}_t) + \lambda_4 Q(F(\tilde{X}(t),X(t))) - \lambda_4 F(X(t),\tilde{X}(t))\\ &\Big[\mathfrak{a}_4\tilde{X}(t) + \mathfrak{a}_2 X(t)\Big].\end{aligned}$$

Next, we recall that for strictly positive constants, $\nu_i > 0$, $i = 1$ to 5, (that we will choose later), we have the following inequalities: $|X\tilde{X}| \leq \frac{1}{\nu_1}Q(X) + \nu_1 Q(\tilde{X})$, $|X(t)X(t-\tau)| \leq \frac{1}{\nu_2}Q(X(t)) + \nu_2 Q(X(t-\tau))$, $|X(t)\tilde{X}(t-\tau)| \leq \frac{1}{\nu_3}Q(X(t)) + \nu_3 Q(\tilde{X}(t-\tau))$, $|\tilde{X}(t)\tilde{U}(t-\tilde{\tau})| \leq \frac{1}{\nu_4}Q(\tilde{X}(t)) + \nu_4 Q(\tilde{U}(t-\tilde{\tau}))$, $|X(t)\tilde{U}(t-\tilde{\tau})| \leq \frac{1}{\nu_5}Q(X(t)) + \nu_5 Q(\tilde{U}(t-\tilde{\tau}))$. Therefore, it follows that the derivative $\dot{V}^\dagger(t)$ satisfies, for almost all $t \geq 0$, the following inequality:

$$\begin{aligned}\dot{V}^\dagger(t) \leq& -[2\lambda_1\mathfrak{a}_1 - \mathfrak{b}_1]Q(\tilde{X}(t)) - [2\mathfrak{a}_6 - \mathfrak{b}_2]Q(X(t)) - \rho_2\lambda_3\mathcal{S}(\tilde{X}_t)\\ &- \rho_2\lambda_2\mathcal{S}(X_t) - \rho_1\lambda_4\mathcal{Y}(\tilde{U}_t) - \Big[\lambda_4 e^{-\rho_1\tilde{\tau}} - \mathfrak{b}_3\Big]Q(\tilde{U}(t-\tilde{\tau}))\\ &- \Big[\lambda_2 e^{-\rho_2\tau} - \mathfrak{b}_4\Big]Q(X(t-\tau)) - \Big[\lambda_3 e^{-\rho_2\tau} - \mathfrak{b}_5\Big]Q(\tilde{X}(t-\tau))\\ &+ \lambda_4 Q(F(\tilde{X}(t),X(t))) - \mathfrak{a}_5\lambda_4 F(X(t),\tilde{X}(t))\tilde{U}(t-\tilde{\tau})\\ &+ X(t)G(X_t,\tilde{X}_t) - \lambda_4 F(X(t),\tilde{X}(t))\Big[\mathfrak{a}_4\tilde{X}(t) + \mathfrak{a}_2 X(t)\Big],\end{aligned} \tag{54}$$

where,

$$\begin{cases}\mathfrak{b}_1 = \lambda_3 + \lambda_4\mathfrak{a}_4^2 + \nu_1|\mathfrak{a}_2\lambda_1 + \mathfrak{a}_7 - \lambda_4\mathfrak{a}_2\mathfrak{a}_4|,\\ \mathfrak{b}_2 = \lambda_2 + \lambda_4\mathfrak{a}_2^2 + \frac{|\mathfrak{a}_2\lambda_1 + \mathfrak{a}_7 - \lambda_4\mathfrak{a}_2\mathfrak{a}_4|}{\nu_1} + \frac{|\mathfrak{a}_8|}{\nu_2} + \frac{|\mathfrak{a}_9|}{\nu_3} + \frac{|\mathfrak{a}_2\mathfrak{a}_5|\lambda_4}{\nu_5},\\ \mathfrak{b}_3 = \lambda_4\mathfrak{a}_5^2 + \nu_4|\mathfrak{a}_3\lambda_1 + \mathfrak{a}_4\mathfrak{a}_5\lambda_4| + \nu_5\lambda_4|\mathfrak{a}_2\mathfrak{a}_5|,\\ \mathfrak{b}_4 = \nu_2|\mathfrak{a}_8|, \quad \text{and,} \quad \mathfrak{b}_5 = \nu_3|\mathfrak{a}_9|.\end{cases} \tag{55}$$

Now we are ready to determine decay conditions that ensure the regional exponential stability of the trivial steady state of the system (33). The terms where F and G are involved in (54) will be used only to determine a subset of the basin of attraction of the trivial steady state of the system (33).

Let us focus on the constant which is multiplied by $Q(\tilde{U}(t-\tilde{\tau}))$ in (54). Using the inequality $|\mathfrak{a}_3\lambda_1 + \mathfrak{a}_4\mathfrak{a}_5\lambda_4| \leq \lambda_1|\mathfrak{a}_3| + \lambda_4|\mathfrak{a}_4\mathfrak{a}_5|$, we notice that the inequality $\lambda_4 e^{-\rho_1\tilde{\tau}} - \mathfrak{b}_3 > 0$ is verified if

$$\lambda_4\Big(e^{-\rho_1\tilde{\tau}} - \mathfrak{a}_5^2 - \nu_4|\mathfrak{a}_4\mathfrak{a}_5| - \nu_5|\mathfrak{a}_2\mathfrak{a}_5|\Big) - \nu_4\lambda_1|\mathfrak{a}_3| > 0. \tag{56}$$

For later use, we set $\mathfrak{d}_1 \triangleq \lambda_4(e^{-\rho_1\tilde{\tau}} - \mathfrak{a}_5^2 - \nu_4|\mathfrak{a}_4\mathfrak{a}_5| - \nu_5|\mathfrak{a}_2\mathfrak{a}_5|) - \nu_4\lambda_1|\mathfrak{a}_3|$.

We deduce that the first decay condition is given by:

$$\mathfrak{a}_5^2 + \nu_4|\mathfrak{a}_4\mathfrak{a}_5| + \nu_5|\mathfrak{a}_2\mathfrak{a}_5| < 1. \tag{57}$$

Indeed, the previous condition is necessary to guarantee that (56) is satisfied. Now, let us select $\nu_4 = \frac{1}{2}|\mathfrak{a}_4|^{-1}$, and $\nu_5 = \frac{1}{2}|\mathfrak{a}_2|^{-1}$, for $\mathfrak{a}_4 \neq 0$ and $\mathfrak{a}_2 \neq 0$. Using the definitions of $\mathfrak{a}_i$'s, ν_4 and ν_5, it follows that the first decay condition (57) is equivalent to

$$(2\tilde{K}e^{-\tilde{\gamma}\tilde{\tau}})^2 + 2\tilde{K}e^{-\tilde{\gamma}\tilde{\tau}} < 1. \tag{58}$$

Remark 5. One notices that we have deliberately chosen $\nu_4 = \frac{1}{2}|\mathfrak{a}_4|^{-1}$, and, $\nu_5 = \frac{1}{2}|\mathfrak{a}_2|^{-1}$, and that these choices are not unique. Indeed, our objective here is to determine a sufficient decay condition that involves only the unhealthy parameters of the permanently dividing subpopulation (for instance, the subpopulation with FLT3-type mutations in AML) which are, $\tilde{K}$, $\tilde{\tau}$ and $\tilde{\gamma}$. For that purpose, we derive a decay condition involving only the parameter $\mathfrak{a}_5$. Therefore, ν_4 and ν_5 are used in order to compensate $\mathfrak{a}_4$ and $\mathfrak{a}_2$. A more general form is given by $\nu_4 = \tilde{\nu}_4|\mathfrak{a}_4|^{-1}$, $\nu_5 = \tilde{\nu}_5|\mathfrak{a}_2|^{-1}$, where $\tilde{\nu}_4 > 0$, and, $\tilde{\nu}_5 > 0$. In this case, the decay condition (58) rewrites as, $(2\tilde{K}e^{-\tilde{\gamma}\tilde{\tau}})^2 + 2(\tilde{\nu}_4 + \tilde{\nu}_5)\tilde{K}e^{-\tilde{\gamma}\tilde{\tau}} < 1$.

Now, notice that a direct consequence of the inequality (58) is that for all $\rho_1 \in (0, \frac{1}{\tilde{\tau}}\ln(\frac{5}{1+4[\mathfrak{a}_5^2+\mathfrak{a}_5]}))$, we get $e^{-\rho_1\tilde{\tau}} - [\mathfrak{a}_5^2 + \mathfrak{a}_5] > \frac{1-[\mathfrak{a}_5^2+\mathfrak{a}_5]}{5} > 0$. Consequently, we deduce that $\mathfrak{d}_1$, which is defined right after (56), and which is now equal to: $\mathfrak{d}_1 = \lambda_4(e^{-\rho_1\tilde{\tau}} - [\mathfrak{a}_5^2 + \mathfrak{a}_5]) - \nu_4\lambda_1|\mathfrak{a}_3|$, satisfies the inequality, $\mathfrak{d}_1 > 0$, for all $\lambda_4 = \frac{\tilde{\lambda}_4\lambda_1\nu_4|\mathfrak{a}_3|}{e^{-\rho_1\tilde{\tau}} - [\mathfrak{a}_5^2+\mathfrak{a}_5]} > 0$, where $\tilde{\lambda}_4 > 1$. Next, using the inequality,

$$\begin{aligned}\Big|F(X(t),\tilde{X}(t))\tilde{U}(t-\tilde{\tau})\Big| \leq& \frac{2|\mathfrak{a}_5|\lambda_4}{\mathfrak{d}_1}Q(F(X(t),\tilde{X}(t)))\\ &+ \frac{\mathfrak{d}_1}{2|\mathfrak{a}_5|\lambda_4}Q(\tilde{U}(t-\tilde{\tau})),\end{aligned}$$

it follows from (54) that,

$$\begin{aligned}\dot{V}^{\dagger}(t) \leq & -[2\lambda_1\mathfrak{a}_1 - \mathfrak{b}_1]Q(\tilde{X}(t)) - [2\mathfrak{a}_6 - \mathfrak{b}_2]Q(X(t)) \\ & - \frac{\mathfrak{d}_1}{2}Q(\tilde{U}(t-\tilde{\tau})) \\ & - \rho_2\lambda_2\mathcal{S}(X_t) - \rho_2\lambda_3\mathcal{S}(\tilde{X}_t) - \left[\lambda_2 e^{-\rho_2\tau} - \mathfrak{b}_4\right]Q(X(t-\tau)) \\ & - \left[\lambda_3 e^{-\rho_2\tau} - \mathfrak{b}_5\right]Q(\tilde{X}(t-\tau)) - \rho_1\lambda_4\mathcal{Y}(\tilde{U}_t) + H(X_t,\tilde{X}_t),\end{aligned} \tag{59}$$

where,

$$\begin{aligned}H\left(X_t,\tilde{X}_t\right) = & \left(\lambda_4 + \frac{2(\mathfrak{a}_5\lambda_4)^2}{\mathfrak{d}_1}\right)Q(F(X(t),\tilde{X}(t))) + X(t)G(X_t,\tilde{X}_t) \\ & - \lambda_4 F(X(t),\tilde{X}(t))\left[\mathfrak{a}_4\tilde{X}(t) + \mathfrak{a}_2 X(t)\right].\end{aligned} \tag{60}$$

Arguing similarly, we select ν_2 and ν_3 that compensate the terms $\mathfrak{a}_8$ and $\mathfrak{a}_9$ (for $|\mathfrak{a}_8| \neq 0$, and $|\mathfrak{a}_9| \neq 0$). For instance, we can consider $\nu_2 = \frac{1}{6|\mathfrak{a}_8|}$ and $\nu_3 = \frac{1}{6|\mathfrak{a}_9|}$. Then, we put, for instance, $\lambda_2 = \lambda_3 = \frac{1}{3}$. We notice that our choices of ν_2 and ν_3 in this case are equivalent to $\mathfrak{b}_4 = \mathfrak{b}_5 = \frac{1}{6}$, and it follows that for all $\rho_2 \in (0, \frac{1}{\tau}\ln(\frac{\lambda_2}{\mathfrak{b}_4}))$, we obtain in this case $e^{-\rho_2\tau} > \frac{2}{3}$. Thus, we end up with[9]

$$\begin{aligned}\mathfrak{d}_2 &\triangleq \lambda_2 e^{-\rho_2\tau} - \mathfrak{b}_4 = \tfrac{1}{3}\left(e^{-\rho_2\tau} - \tfrac{1}{2}\right) > \tfrac{1}{18}, \\ \mathfrak{d}_3 &\triangleq \lambda_3 e^{-\rho_2\tau} - \mathfrak{b}_5 = \tfrac{1}{3}\left(e^{-\rho_2\tau} - \tfrac{1}{2}\right) > \tfrac{1}{18}.\end{aligned} \tag{61}$$

Finally, by selecting $\nu_1 = \lambda_1 = 2$, all the setting parameters involved in the functional $V\dagger$ are now chosen. We conclude that if the decay conditions $\mathfrak{d}_4 \triangleq 2\lambda_1\mathfrak{a}_1 - \mathfrak{b}_1 > 0$, and $\mathfrak{d}_5 \triangleq 2\mathfrak{a}_6 - \mathfrak{b}_2 > 0$, are satisfied, then (59) satisfies for almost all $t \geq 0$,

$$\begin{aligned}\dot{V}^{\dagger}(t) \leq & -3\bar{\mathfrak{d}}V^{\dagger}(X_t,\tilde{X}_t,\tilde{U}_t) - \frac{\mathfrak{d}_4}{2}Q(\tilde{X}(t)) - \frac{\mathfrak{d}_5}{2}Q(X(t)) \\ & - \frac{\mathfrak{d}_1}{2}Q(\tilde{U}(t-\tilde{\tau})) \\ & - \mathfrak{d}_2 Q(X(t-\tau)) - \mathfrak{d}_3 Q(\tilde{X}(t-\tau)) + H(X_t,\tilde{X}_t),\end{aligned}$$

where $\bar{\mathfrak{d}} = \frac{1}{3}\min\{\frac{\mathfrak{d}_4}{2\lambda_1}, \frac{\mathfrak{d}_5}{2}, \rho_1, \rho_2\}$. Next, in Appendix C, we focus on the nonlinear function H, defined right after (59), in order to define a subset of the basin of attraction of the trivial steady state of system (33). By following the arguments given in Appendix C, we prove that in a well-defined region (defined in terms of the initial conditions) we get:

$$\dot{V}^{\dagger}(t) \leq -2\bar{\mathfrak{d}}V^{\dagger}(X_t,\tilde{X}_t,\tilde{U}_t), \quad \text{for almost all} \quad t \geq 0. \tag{62}$$

We integrate this inequality and we obtain for all $t \geq 0$,

$$V^{\dagger}(X_t,\tilde{X}_t,\tilde{U}_t) \leq e^{-2\bar{\mathfrak{d}}t}V^{\dagger}\left(\varphi_{X_t},\varphi_{\tilde{X}_t},\varphi_{\tilde{U}_t}\right). \tag{63}$$

Consequently, we get for all $t \geq 0$, $X^2(t) + \lambda_1\tilde{X}^2(t) \leq 2e^{-2\bar{\mathfrak{d}}t}V^{\dagger}(\varphi_X,\varphi_{\tilde{X}},\varphi_{\tilde{U}})$. We conclude that the trajectories $X(t)$ and $\tilde{X}(t)$ converge exponentially to the trivial steady state of the shifted system, with a decay rate larger than, or equal to, $\bar{\mathfrak{d}}$. By classical arguments, we observe from the second equation in (33) that, since $2\tilde{K}e^{-\tilde{\gamma}\tilde{\tau}} < 1$, $\tilde{U}(t)$ converges exponentially to zero when $X(t)$ and $\tilde{X}(t)$ converge exponentially to the zero.

To summarize, we considered that $\mathfrak{D}$ (or $\mathfrak{E}$) exists and we rewrote the studied system (10) in the form (33). Next, we proved that if the decay conditions ((58), $\mathfrak{d}_4 > 0$, $\mathfrak{d}_5 > 0$) are satisfied, then the trajectories of (33) associated with initial conditions belonging to the set $\mathcal{B}$, converge exponentially to 0-equilibrium of the shifted system (33), with a decay rate larger than, or equal to, $\bar{\mathfrak{d}}$. By explicitly rewriting the decay conditions, we summarize our findings in Section 5 as follows:

[9] Similarly to ν_4 and ν_5 in Remark 5, the choices of ν_2 and ν_3 are not unique (and, similarly, those of λ_2 and λ_3 either). In Example 4, we are going to use different numerical values that also satisfy $\mathfrak{d}_2 > 0$ and $\mathfrak{d}_3 > 0$.

Table 1
Parameters of the unhealthy compartment, and the values of $\tilde{x}_e$ and $\tilde{u}_e$.

$\tilde{\delta}$	$\tilde{\gamma}$	$\tilde{\tau}$	$\tilde{\beta}(m)$	$\tilde{K}$	$\tilde{u}_e$	$\tilde{x}_e$
0.928	0.4	1	$\frac{2.78}{1+3m^2}$	0.2	0.05938567	0.02179864

Table 2
Parameters of the healthy hematopoietic stem cell compartment, and the value of x_e.

δ	γ	τ	$\beta(m)$	x_e
0.168	0.001	0.12	$\frac{0.219}{1+4m^2}$	0.25354595

Theorem 2. *(A) Assume that $\mathfrak{D}$ (resp. $\mathfrak{E}$) exists, then consider the shifted system (33), such that its trivial steady state corresponds to $\mathfrak{D}$ (resp. $\mathfrak{E}$) of (10). If there exist matrices P, S, J, $\overline{P}$ and $\overline{\overline{P}}$, of appropriate dimension, and a positive constant $\tilde{\mathfrak{a}}$, that satisfy the LMI (47), then the trivial steady state of the shifted system (33), which is $\mathfrak{D}$ (resp. $\mathfrak{E}$) of (10), is locally asymptotically stable.*

(B) Assume that system (10) admits a positive steady state $\mathfrak{D}$ (i.e. (25) or (26) in Proposition 1(vii) hold). If

$$\begin{aligned}&\text{(i)} \quad \left(2\tilde{K}e^{-\tilde{\gamma}\tilde{\tau}}\right)^2 + 2\tilde{K}e^{-\tilde{\gamma}\tilde{\tau}} < 1, \\ &\text{(ii)} \quad \tfrac{\mathfrak{b}_1}{4} - \tilde{\alpha}\tilde{\theta}\tilde{x}_e < \tilde{\beta}(x_e + \tilde{\alpha}\tilde{x}_e) + \tilde{\delta}, \\ &\text{(iii)} \quad \tfrac{\mathfrak{b}_2}{2} - \theta x_e < \beta(x_e + \tilde{x}_e) + \delta,\end{aligned} \tag{64}$$

are satisfied, ensuring also that $\mathfrak{d}_2 > 0$ and $\mathfrak{d}_3 > 0$, then $\mathfrak{D}$ is regionally exponentially stable with a decay rate larger than, or equal to, $\bar{\mathfrak{d}}$, and with basin of attraction defined by:

$$\begin{aligned}\mathcal{B}^{\dagger} = \Big\{ & \varphi_x \in \mathcal{C}\left([-\tau,0],\mathbb{R}^+\right), \varphi_{\tilde{x}} \in \mathcal{C}\left([-\tau,0],\mathbb{R}^+\right), \varphi_{\tilde{u}} \in \mathcal{C}\left([-\tilde{\tau},0],\mathbb{R}^+\right) \Big| \\ & V^{\dagger}(\varphi_x - x_e, \varphi_{\tilde{x}} - \tilde{x}_e, \varphi_{\tilde{u}} - \tilde{u}_e) < \overline{V}^{\dagger} \Big\}.\end{aligned} \tag{65}$$

(C) Assume that $\mathfrak{E}$ exists (Proposition 1(ii)), and consider that $\tilde{x}_e = 0$ in (64). If the conditions (64) are satisfied (for $\tilde{x}_e = 0$), then $\mathfrak{E}$ of (10) is regionally exponentially stable with a decay rate $\mathfrak{d}$ and basin of attraction defined by (65), where we consider now that $\tilde{x}_e = \tilde{u}_e = 0$ in (65).

Example 4. In this example, we assume that $\tilde{\alpha} = 5$. For the unhealthy compartment, we consider the parameters given in Table 1, while for the healthy case we consider the parameters of Table 2.

We want to investigate the stability properties of the dormancy steady state: $\mathfrak{D} = (\tilde{x}_e, \tilde{u}_e, x_e)$, where, $\tilde{x}_e = 0.0217$, $\tilde{u}_e = 0.0593$, and $x_e = 0.2535$. Obviously, if the decay conditions (64) are satisfied, then the LMI (47) admits a solution.

We check that the decay conditions (64) are verified:

$$\begin{aligned}&\text{(i)} \quad 1 - 2\tilde{K}e^{-\tilde{\gamma}\tilde{\tau}} - \left(2\tilde{K}e^{-\tilde{\gamma}\tilde{\tau}}\right)^2 = 0.659979347 > 0, \\ &\text{(ii)} \quad \tilde{\beta}(x_e + \tilde{\alpha}\tilde{x}_e) + \tilde{\delta} - \left(\tfrac{\mathfrak{b}_1}{4} - \tilde{\alpha}\tilde{\theta}\tilde{x}_e\right) = 0.987350196 > 0, \\ &\text{(iii)} \quad \beta(x_e + \tilde{x}_e) + \delta - \left(\tfrac{\mathfrak{b}_2}{2} - \theta x_e\right) = 0.000149333 > 0,\end{aligned} \tag{66}$$

where we consider: $\lambda_1 = 2$, $\lambda_2 = \lambda_3 = 0.261780$, $\lambda_4 = 2.205796$, $\tilde{\lambda}_4 = 2$, $\nu_1 = 2$, $\nu_2 = \frac{1}{4|\mathfrak{a}_8|} = 1.301858$, $\nu_3 = \frac{1}{4|\mathfrak{a}_9|} = 1.736024$, $\nu_4 = \frac{1}{2|\mathfrak{a}_4|} = 0.302151$, $\nu_5 = \frac{1}{2|\mathfrak{a}_2|} = 7.374022$, $\rho_1 = \frac{1}{10\tilde{\tau}}\ln(\frac{5}{1+4(\mathfrak{a}_5^2+\mathfrak{a}_5)}) = 0.075074$ and $\rho_2 = \frac{1}{10\tau}\ln(\frac{\lambda_2}{\mathfrak{b}_4}) = 0.038369$. For these numerical values, we check that $\mathfrak{d}_2 = \mathfrak{d}_3 = 0.010577 > 0$. Therefore, according to Theorem 2, the dormancy steady state, $\mathfrak{D} = (0.0217, 0.0593, 0.2535)$, is regionally exponentially stable, as illustrated in Fig. 7. This example will be revisited in the next section, in the practical situation of therapeutic strategies.

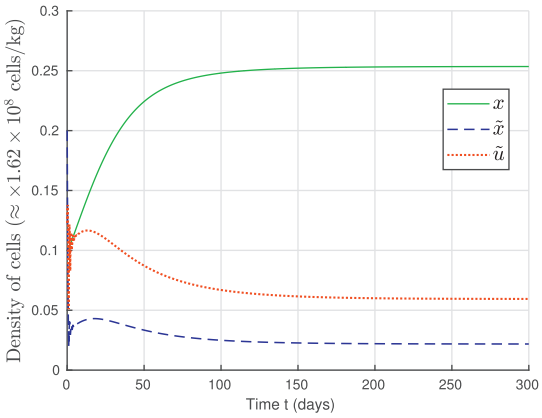

Fig. 7. Trajectories of the system of the numerical Example 4 (Tables 1 and 2). In this case, the dormancy steady state $\mathfrak{D}$ exists, such that $\tilde{x}_e = 0.0217$, $\tilde{u}_e = 0.0593$. The sufficient local stability conditions given in *Theorem 2(B)* are satisfied, as shown in (66), and the trajectories of the system converge exponentially to $\mathfrak{D}$.

Table 3
The set of initial (i.e. before treatment) parameters of the unhealthy compartment.

$\tilde{\delta}$	$\tilde{\gamma}$	$\tilde{\tau}$	$\tilde{\beta}(m)$	$\tilde{K}$	$\tilde{\alpha}$
0.25	0.1	0.2	$\frac{2.78}{1+m^3}$	0.55	0.8

6. Concluding comments on the findings and possible therapeutic strategies oriented towards cancer dormancy

A first remark is that CSC dormancy probably results from complex relationships between the different biological parameters involved in this process, that are difficult to elicit, let alone to be understood. This observation concerns the stability properties (decay conditions in Theorem 2), but also the conditions of existence of dormancy (Proposition 1(vii)), along with the role of the sensitivity parameter $\tilde{\alpha}$. This should lead us to develop further the mathematical framework sketched here, in order to help us understand the mechanisms behind dormancy. In the current section, we emphasize the main case of hematopoiesis and AML. In fact, experiments on fresh blood samples of patients with hyperleukocytosis may allow to identify the apoptosis and differentiation rates in the specific case of AML. However, there is no immediate prospect for estimating the proliferation functions $\tilde{\beta}$ and β, as well as the fast self-renewing parameter $\tilde{K}$. In addition, cancer dormancy is not easily traceable at the current time, since clinical manifestation of cancer is detectable only when tumor size exceeds a given threshold. Thus, model identification is a highly topical open issue, and our attention is only focused on the qualitative asymptotic behavior of our model, which is otherwise in line with the biological observations in this field. Nevertheless, as a first step, the analysis that we performed throughout this paper reveals that our theoretical results may suggest some therapeutic guidelines to eradicate aggressive CSCs ($\mathfrak{E}$), or to bring them to dormancy ($\mathfrak{D}$), as discussed in the sequel.

(1) Towards the adoption of a common therapeutic strategy to yield states $\mathfrak{D}$ and $\mathfrak{E}$? It cannot be claimed that convergence to the steady state $\mathfrak{D}$ and the steady state $\mathfrak{E}$ should share the same therapeutic roadmap, since a crucial difference lies in their conditions of existence. For instance, $\mathfrak{E}$ exists even if $\tilde{\delta} > \frac{2e^{-\tilde{\gamma}\tilde{\tau}}-1}{1-2\tilde{K}e^{-\tilde{\gamma}\tilde{\tau}}}\tilde{\beta}(0)$ (see Proposition 1), while the reverse situation is required in order to allow for the existence of dormancy $\mathfrak{D}$, in addition to other conditions. We recall that in our system, the conditions of existence of the steady states of interest are a type of *red lines*, that must not be crossed when elaborating a treatment strategy.

On the other hand, when we focus on the stability conditions, wondering how therapeutic actions can make the biological system go into the direction of the decay conditions (64), we realize that the respective decay conditions of $\mathfrak{D}$ and $\mathfrak{E}$ are substantially similar. More precisely, our sufficient stability conditions suggest that the biological parameters that can be targeted in order to satisfy (64), in either of the two states $\mathfrak{D}$ or $\mathfrak{E}$, are similar (but not identical). In this sense, we can state that a common therapeutic strategy for $\mathfrak{D}$ and $\mathfrak{E}$ can be proposed. So, in light of the existing therapies and recent clinical trials that highlight novel effective molecules as potential drugs in AML, we briefly discuss how a combined therapy – mostly composed of targeted therapies and standard chemotherapy – may satisfy the theoretical conditions (64).

First, we observe that the condition *(B-i)* in Theorem 2 provides a restriction on the dynamics of over-proliferating cells, since $\tilde{K}$, $\tilde{\gamma}$ and $\tilde{\tau}$ are involved. Satisfying the previous condition relies in increasing the product $\tilde{\gamma}\tilde{\tau}$, and decreasing $\tilde{K}$. Increasing $\tilde{\gamma}\tilde{\tau}$ means that we extend the average duration of the cell cycle $\tilde{\tau}$ and/or increase the apoptosis rate $\tilde{\gamma}$ in the population of unhealthy cells. Leukemic cells may be targeted by drugs such as quizartinib (AC220, Zarrinkar, 2009) or erlotinib (Lainey et al., 2011) to increase $\tilde{\tau}$, while cytosine arabinoside can be used to increase the apoptosis rate $\tilde{\gamma}$. Moreover, quizartinib can be used to decrease the fast self-renewal rate $\tilde{K}$. In fact, $\tilde{K}$ is expected to be the hardest parameters to modify in practice, due to preexisting mutations in epigenetic control genes (DNMT3A, TET2). However, new *FLT3 inhibitors*, such as midostaurin,[10] have achieved good performance (see the recent quantitative results provided in Stone et al., 2017) and are now approved for use along with chemotherapy to target leukemic cells in AML.

Next, in the conditions *(B-ii)* and *(B-iii)* of Theorem 2, the targets can be the parameters δ and $\tilde{\delta}$ (mainly $\tilde{\delta}$, since it is the unhealthy parameter) that appear in the right hand sides of the corresponding inequalities. We recall that $\tilde{\delta}$ includes the death rate and the differentiation rate of unhealthy resting cells. In practice, increasing $\tilde{\delta}$ means that we should increase the differentiation rates, which can be achieved in the case of leukemia by infusing dasatinib (Lainey et al., 2011), that targets most of the tyrosine kinases including the c-KIT gene. In fact, it was thought that drugs promoting re-differentiation of CSCs in many cancers are not effective in the specific case of AML. However, this therapeutic option has been relaunched recently after successful clinical trials, where *dihydroorotate dehydrogenase (DHODH) inhibitors* restored differentiation of leukemic cells in AML (Sykes et al., 2016). Finally, increasing $\beta(0)$ and $\tilde{\beta}(0)$ can be performed by using G-CSF molecules (Foley et al., 2006). These are the main common targets shared by $\mathfrak{D}$ and $\mathfrak{E}$.

(2) Constraints and spillover risks of CSCs eradication: Increasing the parameters $\tilde{\delta}$, $\tilde{\gamma}$ and $\tilde{\tau}$ (using some of the previously mentioned molecules or their equivalent), promotes the existence of the state $\mathfrak{E}$, together with its stability. However, it may exclude the steady state $\mathfrak{D}$, by violating its conditions of existence. Furthermore, an excessive therapy that affects also healthy cells leads, theoretically, to the extinction of all the cells (*Theorem 1*). At the other extreme, insufficient drug dose might not successfully stop CSCs from overproliferation (when $2\tilde{K}e^{-\tilde{\gamma}\tilde{\tau}} > 1$). The overproliferating behavior may be worsened by CSC resistance to drugs. Thus, dormancy $\mathfrak{D}$ appears as a delicate intermediate equilibrium between the cancer progression and CSC eradication.

(3) Specific constraints related to dormancy: In the *common strategy* that aims to satisfy the condition (64), we noticed that drugs have to increase the product $\tilde{\gamma}\tilde{\tau}$. On the other hand, we recall

[10] Midostaurin is a multi-targeted protein kinase inhibitor, which can be active against oncogenic CD135 (FMS-like tyrosine kinase 3 receptor, FLT3) (Döhner et al., 2015; Stone et al., 2017).

from Proposition 1(vii) that the condition $1 < 2e^{-\tilde{\gamma}\tilde{\tau}}$ is necessary for the existence of $\mathfrak{D}$. Thus, the therapy action in this case has to take into account this supplementary condition. We infer from this remark that the probability to achieve the dormancy steady state $\mathfrak{D}$ by using the classical strategies that consist in giving the maximum tolerated dose of drugs during the treatment period (Enderling, 2013), is therefore very low. Indeed, since a high dose is expected to yield $1 > 2e^{-\tilde{\gamma}\tilde{\tau}}$, the condition of existence of $\mathfrak{D}$ is then violated. The multiple restrictions on the biological parameters listed in *Proposition 1* show that the existence of $\mathfrak{D}$ is more difficult to achieve than the existence of $\mathfrak{E}$. However, we suggest that infusing G-CSF molecules appears to favor the existence of a dormancy steady state, since increasing (relatively) $\beta(0)$ seems to go in the right direction in order to satisfy both the existence and the stability conditions of $\mathfrak{D}$.

(4) The suggestion of therapeutic strategies that achieve dormancy: In light of the above discussion, we propose to implement what can be considered as a simple theoretical therapeutic strategy that aims to achieve a stable dormancy steady state. More precisely, we consider an hematopoietic system with the clinical symptoms that we expect when facing some overproliferating malignant hemopathies. This ranges from a blockade in differentiation mechanisms to the survival of abnormal cells, along with a high rate of self-renewal activity. We will in fact check that in the absence of adequate treatment, the unhealthy population will proliferate abundantly. Then, in a second time, our objective is to stabilize the total cell density, through multiple drug infusions of a combined therapy that is in line with our theoretical results (i.e. the decay conditions in *Theorem 2*). In other words, we aim to bring the hematopoietic system from an initial abnormal overproliferating state into a dormant stable steady state. For that purpose, let us assume that the initial parameters of the unhealthy compartment are those given in Table 3. In fact, we have deliberately chosen an intuitive set of parameters that matches specific dysfunctions in overproliferating malignant hemopathies (particularly the condition $2\tilde{K}e^{-\tilde{\gamma}\tilde{\tau}} > 1$).

On the other hand, we assume that the parameters of the healthy compartment are those given in Example 4, and we consider that the therapy to be administrated has a negligible effect on ordinary cells.

In medical practice, usually the hematopoietic system is targeted through chemotherapy or targeted therapy (a combination of two or three drugs), sometimes infused along with a complementary treatment. All these drugs have in fact molecular targets (e.g. dasatinib targets BCR/Abl, Src, ephrin receptors, c-Kit and many other tyrosine kinases), that result in a modification of some biological mechanisms (e.g. generally, dasatinib increases proliferation, and differentiation in AML (Fang et al., 2013). It should be borne in mind that the functional effect resulting from the molecular action of the infused drugs, varies in practice according to several facts (for instance, the buildup of many types of mutations by some individuals). However, when we put aside all the intermediate complications that may exist in practice, we can take a shortcut that associates to each infused drug its most likely action on one or several biological functions (that are: differentiation, apoptotis, and so on), with a certain amount of confidence. Thus, we can roughly state from medical practice some major families of molecules that can be used in the case of AML or other cancers, according to their expected effect on the biological functionalities.

Remark 6. (i) One notices that some molecules in Table 4 are expected to modify more than one model parameter. For instance, the DHODH inhibitor, which is a differentiation re-activator, may decrease $\tilde{K}$ and increase $\tilde{\delta}$, since both actions seem to promote a return into normal differentiation. (ii) The volasertib (recognized as orphan drug for AML since 2014), belongs to the family of *Polo-like kinase (Plk) inhibitors*. It can be used in the treatment of AML to promote apoptosis and cell cycle arrest (see for instance Brandwein, 2015). In fact, the list of drugs given in Table 4 is not exhaustive and can be enlarged, for instance, to: *histone deacetylase (HDAC) inhibitors* (vorinostat and panobinostat), and the family of *aurora kinase inhibitors* (AZD115).

Table 4
Here we associate the most likely (clinically established) effect of some advanced drugs/molecules on the biological features of the hematopoietic system, in the specific case of AML (without focusing neither on the molecular mechanisms behind each drug action, or on the possible mutual interactions that may exist between drugs within some combinations). The case of the sensitivity parameter $\tilde{\alpha}$ is discussed later, in Remark 7.

Fast self-renewing ($\tilde{K}$)	Quizartinib, midostaurin Dihydroorotate dehydrogenase (DHODH) inhibitors
Apoptosis ($\tilde{\gamma}$)	Daunorubicin, cytosine arabinoside, volasertib
Differentiation ($\tilde{\delta}$)	Dihydroorotate dehydrogenase (DHODH) inhibitors
Cell cylce dur. ($\tilde{\tau}$)	Quizartinib, erlotinib, volasertib

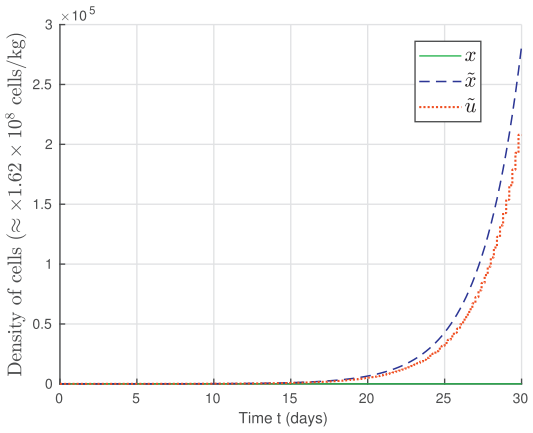

Fig. 8. Trajectories of the system for the (non-treated) model parameters of Table 3.

Now, we observe that the biological parameters considered in Table 3 imply that $2\tilde{K}e^{-\tilde{\gamma}\tilde{\tau}} = 1.078$. It follows that, theoretically, if AML is not treated, unhealthy cells will invade the bone marrow and possibly the bloodstream. In Fig. 8, we illustrate the evolution of cell densities for the selected model parameters, where we observe the unbounded proliferation of unhealthy cells.

Remark 7. We expect that $\tilde{\alpha}$ is less than 1 before therapy, then it starts to increase when therapy is applied (an immunostimulating effect of cytotoxic drugs, elicited e.g. in Zitvogel et al., 2008; Zitvogel et al., 2006), and then greater than 1 when the immune system has learnt to counter the dodges of cancer cells (such as hiding their tumor antigens or achieving inactivation of antibodies, e.g. by glycosylation), or when the reduction of the tumor burden has made immune cells proportionally more efficient in their encounters with cancer cells, or also when successful immunotherapy is used to directly target cancer cells.

Actually, the elaboration of an *optimal* therapeutic strategy[11] is beyond the scope of this work. Here, we are suggesting a theoretical therapeutic strategy, that can be based on some suitable combination of drugs (listed in Table 4, or others similar ones). We assume that the resulting evolution patterns of the biological model parameters are those illustrated in Fig. 9. In fact, we can distin-

[11] The optimal therapy requires the determination of the best infusion planning, that takes into account drug toxicity and other practical considerations (e.g. how the doses of each drug type are spread over the duration of the therapy). These points deserve a separated study.

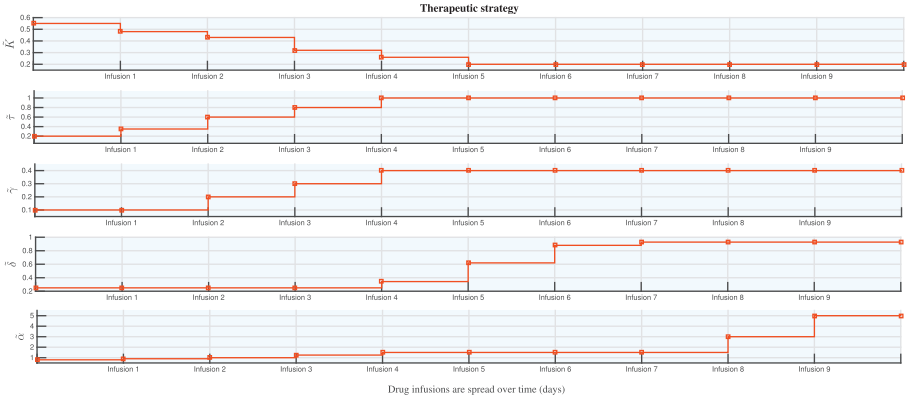

Fig. 9. An illustrative therapeutic strategy that gradually modifies five model parameters, using adequates drugs: this can be achieved using a mixture of standard chemotherapy or targeted therapies, along with complementary molecules and/or immunotherapeutic actions.

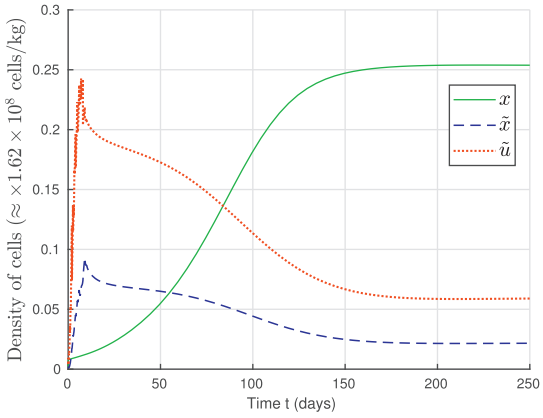

Fig. 10. The evolution of the total densities of healthy and unhealthy cells (resp. $x(t)$ and $\tilde{x}(t)$) and $\tilde{u}(t)$, when we apply the theoretical therapeutic strategy illustrated in Fig. 9. If we do not change the parameter values, the model behaves as in Fig. 8 (i.e. CSCs overproliferate). However, in the case of treated cancer, the trajectories converge to a dormancy stable steady state, under the effect of the suggested therapy.

guish between two evolution trends, nested within one another as follows:

(1) The first series of infusions aims to decrease $\tilde{K}$ (fast self-renewing rate), to increase $\tilde{\tau}$ (cell-cycle duration), and to increase $\tilde{\gamma}$ (apoptosis rate). It is worth mentioning that the direction of the change in the model parameters (i.e. by increasing/decreasing the model parameters values) is in line with the observed effect of the drugs listed in Table 3. This treatment phase is expected to limit the expansion of CSCs. We also assume that the first treatment phase is accompanied by a slight increase of the value of $\tilde{\alpha}$ (see Remark 7).

(2) The second phase of the treatment aims, on the one hand, to maintain the trend given for the parameters ($\tilde{K}$, $\tilde{\tau}$, $\tilde{\gamma}$), and on the other hand, to reactivate the differentiation of unhealthy cells (using DHODH inhibitors, for instance) and to increase the sensitivity parameter $\tilde{\alpha}$ with more virulence than in the first series of infusions (e.g. using a suitable immunotherapeutic action, Remark 7).

Remark 8. It seems legitimate to wonder whether the reactivation of differentiation of CSCs is a good strategy to fight cancer. The answer is argued for instance in Enderling (2013), where it is explained how CSCs can initiate and regenerate cancers, while differentiated cancer cells (called CCs Enderling, 2013) will inevitably die out (see the section *"Cancer stem cells and non-stem cancer cells"*, Enderling, 2013). Thus, promoting the differentiation of CSCs into CCs appears as a sustainable way to both limit cancer progression, and avoid the escape from cancer dormancy.

Now, let us assume that an adequate combination of drugs has been fixed. We can highlight one suggestion among other possibilities, in which we propose:

①a shock treatment through chemotherapy that promotes apoptosis $\tilde{\gamma}$ and cell arrest $\tilde{\tau}$ (using volasertib for both objectives), and targeting $\tilde{K}$ using AC220 (which has also a suitable effect on cell arrest $\tilde{\tau}$),

② followed by a more differentiation-oriented treatment (using drugs based on DHODH inhibitors) and mitotic/proliferation inhibition of unhealthy cells (possibly using some immunotherapy-based drugs, or vincristine, see also Saygin and Carraway, 2017).

We aim through the selected therapy to achieve an evolution pattern of the model parameters as close as possible to the idealistic ones given in Fig. 9.

Remark 9. The treatment protocol that we suggest have many similarities with classical methods in AML therapeutics (Saygin and Carraway, 2017). We can mention in particular the **3+7** most famous strategy, which is also based on two main separated phases (7 days of intensive induction through cytarabine, plus 3 days of an anthracycline (Saygin and Carraway, 2017), and then possibly followed by consolidation chemotherapy and hematopoietic cell transplant (Döhner et al., 2015; Saygin and Carraway, 2017).

Next, we apply the therapeutic strategy given in Fig. 9 to our model, starting the first infusion at $t = 1$ day, and considering a fixed treatment step of 1 day between successive infusions (another choice may be envisaged if needed). One notices that the model parameters after *Infusion* 9 are those given in Example 4, for which the decay conditions (64) of Theorem 2 are satisfied.

The evolution of the ordinary and mutated cell densities is shown in Fig. 10. It is worth mentioning that in practice, the treatment of AML is spread over several separated phases. For instance, in the recent experimental work (Stone et al., 2017), an AML (FLT3-type) therapy based on midostaurin and chemotherapy, has been separated into two *induction phases*, a *consolidating phase* and *maintenance phase* (59% of patients that have undergone the previously mentioned therapeutic protocol, then underwent bone marrow transplant, have reached the complete remission state (Stone et al., 2017). Similarly, in our example, we assume that after *Infusion* 9, a consolidating and a maintenance

phases continue so as to correct, adjust, strengthen, and fortify the desired dormancy state of the hematopoietic system (which is the state described by the set of parameters of *Infusion* 9).

We conclude this work by referring to Table 1 in Saygin and Carraway (2017), which summarizes a number of emerging promising AML therapies, that open up other possibilities to act on cancerous hematopoietic systems. Many of these strategies can in fact be implemented and discussed within the modeling and analysis framework that we introduced in our current work. It is worth mentioning that the addition of midostaurin to chemotherapy resulted in a 22% lower risk of death among patients, in comparison to another more classical treatment (see Stone et al., 2017). Notice that, most of the molecules listed in Saygin and Carraway (2017) (and the references therein) are in early phases of development and trials, but they participate greatly, as well as many multidisciplinary works, to nourish this hope of moving towards systematic treatments for cancer, in general, and leukemia, in particular.

Acknowledgment

We would like to thank the A.E. and the reviewers of JTB for their valuable comments. We also thank professors P. Pepe and M. Adimy, referees of the PhD thesis of W. Djema, for the stimulating discussions we had on the topic. This work was supported by the DIGITEO Project ALMA3 and the iCODE project funded by the IDEX Paris-Saclay, ANR-11-IDEX-0003-02.

Appendix A. Proof of Theorem 1 (cell extinction)

Simple calculations show that the derivative of $\mathcal{W}$, defined in (28), along the trajectories of (10), satisfies, for almost all $t\geq 0$,

$$\begin{aligned}\dot{\mathcal{W}}(t) =&\Big[-\tilde{\delta}+(\psi_1-1)\tilde{\beta}(x(t)+\tilde{\alpha}\tilde{x}(t))\Big]\tilde{x}(t)\\ &-\Big[\psi_1(e^{-\rho_1^*\tilde{\tau}}-2\tilde{K}e^{-\tilde{\gamma}\tilde{\tau}})-2(1-\tilde{K})e^{-\tilde{\gamma}\tilde{\tau}}\Big]\tilde{u}(t-\tilde{\tau})\\ &-[\delta+(1-\psi_2)\beta(x(t)+\tilde{x}(t))]x(t)\\ &-\psi_1\rho_1^*\int_{t-\tilde{\tau}}^{t}e^{\rho_1^*(\ell-t)}\tilde{u}(\ell)d\ell\\ &-(\psi_3e^{-\rho_2^*\tau}-1)2e^{-\gamma\tau}\beta(x(t-\tau)+\tilde{x}(t-\tau))x(t-\tau)\\ &-\psi_2\rho_2^*\int_{t-\tau}^{t}e^{\rho_2^*(\ell-t)}\beta(x(\ell)+\tilde{x}(\ell))x(\ell)d\ell.\end{aligned}$$

Now, according to (29), the conditions $2\tilde{K}e^{-\tilde{\gamma}\tilde{\tau}}<1$ and $\psi^*>0$ are satisfied. It follows that for all $\rho_1^*\in(0,\frac{1}{\tilde{\tau}}\ln(\frac{k}{1+2(k-1)\tilde{K}e^{-\tilde{\gamma}\tilde{\tau}}}))$, where $k>1$ is a constant that we will select later, we get $0<\frac{1-2\tilde{K}e^{-\tilde{\gamma}\tilde{\tau}}}{k}<e^{-\rho_1\tilde{\tau}}-2\tilde{K}e^{-\tilde{\gamma}\tilde{\tau}}<1-2\tilde{K}e^{-\tilde{\gamma}\tilde{\tau}}$. On the other hand, using the definition of ψ_1, we can readily check that:

$$\psi_1\big(1-2\tilde{K}e^{-\tilde{\gamma}\tilde{\tau}}\big)-2\big(1-\tilde{K}\big)e^{-\tilde{\gamma}\tilde{\tau}}>0.$$

Therefore, we can notice that for all $k\in(1,\frac{(1-2\tilde{K}e^{-\tilde{\gamma}\tilde{\tau}})\psi_1}{2(1-\tilde{K})e^{-\tilde{\gamma}\tilde{\tau}}})$, the constant:

$$\bar{k}=\psi_1\left(\frac{1-2\tilde{K}e^{-\tilde{\gamma}\tilde{\tau}}}{k}\right)-2\big(1-\tilde{K}\big)e^{-\tilde{\gamma}\tilde{\tau}},$$

is strictly positive. Next, since $\tilde{\beta}$ is decreasing, and using the fact that $\psi_{11}>1$, it follows that $(\psi_{11}-1)\tilde{\beta}(x(t)+\tilde{\alpha}\tilde{x}(t))\leq(\psi_{11}-1)\tilde{\beta}(0)$. From the previous intermediate results, we conclude that for all $t\geq 0$, $-\tilde{\delta}+(\psi_1-1)\tilde{\beta}(x(t)+\tilde{\alpha}\tilde{x}(t))\leq\psi_{12}\tilde{\beta}(x(t)+\tilde{\alpha}\tilde{x}(t))$, where, $\psi_{12}<0$. Now, we assume that the third decay condition, $\delta>(2e^{-\gamma\tau}-1)\beta(0)$, is satisfied, and we put $\psi_3=\frac{2\beta(0)+(\delta+\beta(0))e^{\gamma\tau}}{4\beta(0)}$. Therefore, it is easy to check that, in this case, we have $\psi_3\in(1,\frac{\delta+\beta(0)}{2\beta(0)}e^{\gamma\tau})$. It follows that $\delta+(1-\psi_2)\beta(0)$ is positive. For later use we denote $\delta^*=\delta+(1-\psi_2)\beta(0)$. Next, by selecting $\rho_2^*=\frac{1}{2\tau}\ln(\frac{2\psi_3}{\psi_3+1})>0$, we deduce that $\psi_3e^{-\rho_2\tau}-1$ is positive. For later use we denote $\rho^*=\psi_3e^{-\rho_2^*\tau}-1$. We conclude that $\dot{\mathcal{W}}(t)$ satisfies, for almost all $t\geq 0$,

$$\begin{aligned}\dot{\mathcal{W}}(t)\leq&\psi_{12}\tilde{\beta}(x(t)+\tilde{\alpha}\tilde{x}(t))\tilde{x}(t)-\psi_1\rho_1\int_{t-\tilde{\tau}}^{t}e^{\rho_1(\ell-t)}\tilde{u}(\ell)d\ell\\ &-\bar{k}\tilde{u}(t-\tilde{\tau})-2\rho^*e^{-\gamma\tau}\beta(x(t-\tau)+\tilde{x}(t-\tau))x(t-\tau)\\ &-\delta^*x(t)-\psi_2\rho_2\int_{t-\tau}^{t}e^{\rho_2(\ell-t)}\beta(x(\ell)+\tilde{x}(\ell))x(\ell)d\ell,\end{aligned}\tag{A.1}$$

where, $\psi_{12}<0$, $\bar{k}>0$, $\delta^*>0$, and, $\rho^*>0$. By integrating the previous inequality (A.1), we deduce that the functional $\mathcal{W}$ is bounded over $[0,+\infty)$. From the definition of $\mathcal{W}$, it follows that for all $t\geq 0$, the trajectories $\tilde{x}(t)$ and $x(t)$ are bounded by, respectively, the positive constants $\tilde{x}_s$ and x_s. A direct consequence is that for almost all $t\geq 0$,

$$\begin{aligned}\dot{\mathcal{W}}(t)\leq&\psi_{12}\tilde{\beta}(x_s+\tilde{\alpha}\tilde{x}_s)\tilde{x}(t)-\psi_1\rho_1\int_{t-\tilde{\tau}}^{t}e^{\rho_1(\ell-t)}\tilde{u}(\ell)d\ell\\ &-\delta^*x(t)-\psi_2\rho_2\int_{t-\tau}^{t}e^{\rho_2(\ell-t)}\beta(x(\ell)+\tilde{x}(\ell))x(\ell)d\ell.\end{aligned}$$

We conclude that for almost all $t\geq 0$, we have,

$$\dot{\mathcal{W}}(t)\leq-\psi_4\mathcal{W}(\tilde{x}_t,\tilde{u}_t,x_t),\tag{A.2}$$

where $\psi_4=\min\{-\psi_{12}\tilde{\beta}(x_s+\tilde{\alpha}\tilde{x}_s),\delta^*,\rho_1^*,\rho_2^*\}>0$. Now, by integrating the inequality (A.2), we deduce that for all $t\geq 0$,

$$\mathcal{W}(\tilde{x}_t,\tilde{u}_t,x_t)\leq e^{-\psi_4 t}\mathcal{W}(\varphi_{\tilde{x}},\varphi_{\tilde{u}},\varphi_x).\tag{A.3}$$

It follows from the definition of $\mathcal{W}$ that $\tilde{x}$ and x converge exponentially to zero with a decay rate larger than, or equal to, ψ_4. From the second equation in (10), we note that the linearity in $\tilde{u}$ and the fact that $2\tilde{K}e^{-\tilde{\gamma}\tilde{\tau}}<1$, imply that $\tilde{u}$ converges exponentially to the 0-equilibrium of the shifted system when $\tilde{x}$ and x also converge exponentially to zero. This concludes the proof of Theorem 1.

Appendix B. Determining $\mathfrak{s}$, $\tilde{\mathfrak{s}}$, $\mathfrak{m}$, and $\tilde{\mathfrak{m}}$, in (37) and (38)

Since R and $\tilde{R}$ have similar forms, we prove the desired results only for R. Using the expression of β given in (1), we rewrite for all $\mathfrak{e}>0$ and $\mathfrak{z}>-\mathfrak{e}$,

$$R(\mathfrak{z})=\beta(0)\left(\frac{1}{1+b(\mathfrak{z}+\mathfrak{e})^n}-\frac{1}{1+b\mathfrak{e}^n}\right)-\theta\mathfrak{z}.\tag{B.1}$$

Obviously, when $|\mathfrak{z}|>1$, we have

$$\frac{|R(\mathfrak{z})|}{|\mathfrak{z}|}\leq\frac{2\beta(0)+|\theta|}{|\mathfrak{z}|}\leq 2\beta(0)+|\theta|.\tag{B.2}$$

To address the case where $|\mathfrak{z}|\leq 1$ for all $\mathfrak{z}>-\mathfrak{e}$ and $\mathfrak{e}>0$, we consider first the function:

$$\rho^\dagger(\mathfrak{z})=\frac{1}{1+b(\mathfrak{z}+\mathfrak{e})^n}-\frac{1}{1+b\mathfrak{e}^n}=\frac{b[\mathfrak{e}^n-(\mathfrak{z}+\mathfrak{e})^n]}{q(\mathfrak{z})},$$

where $q(\mathfrak{z})=[1+b(\mathfrak{z}+\mathfrak{e})^n](1+b\mathfrak{e}^n)$. Using,

$$(\mathfrak{z}+a)^n-a^n=na^{n-1}\mathfrak{z}+n(n-1)\int_0^{\mathfrak{z}}\int_a^{a+l}m^{n-2}dmdl,$$

we deduce that,

$$\rho^\dagger(\mathfrak{z})=-nb\mathfrak{e}^{n-1}\frac{\mathfrak{z}}{q(\mathfrak{z})}+\mathfrak{C}(\mathfrak{z}),\tag{B.3}$$

where $\mathfrak{C}(\mathfrak{z})=-nb(n-1)\frac{1}{q(\mathfrak{z})}\int_0^{\mathfrak{z}}\int_0^{\ell}(m+\mathfrak{e})^{n-2}dmd\ell$. We ease the notation by considering $h=1+b\mathfrak{e}^n$. Then, by noticing that $\frac{1}{q(\mathfrak{z})}=$

$\frac{1}{h}(\rho^\dagger(\mathfrak{z})+\frac{1}{h})$, it follows that $\rho^\dagger(\mathfrak{z})=-nb\mathfrak{e}^{n-1}(\frac{\rho^\dagger(\mathfrak{z})}{h}+\frac{1}{h^2})\mathfrak{z}+\mathfrak{C}(\mathfrak{z})$. Consequently,

$$\rho^\dagger(\mathfrak{z})=-\frac{nb\mathfrak{e}^{n-1}}{h^2}\mathfrak{z}+\mathfrak{C}(\mathfrak{z})-\frac{nb\mathfrak{e}^{n-1}}{h}\rho^\dagger(\mathfrak{z})\mathfrak{z}. \tag{B.4}$$

We recall that, by definition, $\theta=\beta'(\mathfrak{e})=\beta(0)\frac{nb\mathfrak{e}^{n-1}}{h^2}$. Therefore,

$$\rho^\dagger(\mathfrak{z})+\frac{\theta}{\beta(0)}\mathfrak{z}=\mathfrak{C}(\mathfrak{z})-\frac{nb\mathfrak{e}^{n-1}}{h}\rho^\dagger(\mathfrak{z})\mathfrak{z}. \tag{B.5}$$

On the other hand, observe that (B.1) is equivalent to $R(\mathfrak{z})=\beta(0)[\rho^\dagger(\mathfrak{z})-\frac{\theta}{\beta(0)}\mathfrak{z}]$. By combining the last equality with (B.5), we get the intermediate consequence,

$$\frac{R(\mathfrak{z})}{\beta(0)}=\mathfrak{C}(\mathfrak{z})-\frac{nb\mathfrak{e}^{n-1}}{h}\rho^\dagger(\mathfrak{z})\mathfrak{z}. \tag{B.6}$$

Now, we readily check that

$$|\mathfrak{C}(\mathfrak{z})|\le\frac{nb(n-1)}{q(\mathfrak{z})}(|\mathfrak{z}|+\mathfrak{e})^{n-2}\frac{\mathfrak{z}^2}{2}. \tag{B.7}$$

From (B.3) we deduce that $|\rho^\dagger(\mathfrak{z})|\le\frac{nb\mathfrak{e}^{n-1}}{q(\mathfrak{z})}|\mathfrak{z}|+|\mathfrak{C}(\mathfrak{z})|$. Using (B.7), it follows that

$$\left|\mathfrak{z}\rho^\dagger(\mathfrak{z})\right|\le\frac{nb\mathfrak{e}^{n-1}}{q(\mathfrak{z})}\mathfrak{z}^2+\frac{nb(n-1)}{2q(\mathfrak{z})}(|\mathfrak{z}|+\mathfrak{e})^{n-2}|\mathfrak{z}|^3. \tag{B.8}$$

Consequently, from (B.6), and using (B.7) and (B.8), we obtain the upper bound,

$$\begin{aligned}\frac{|R(\mathfrak{z})|}{\beta(0)}\le&\frac{(nb)^2(n-1)\mathfrak{e}^{n-1}}{2hq(\mathfrak{z})}(|\mathfrak{z}|+\mathfrak{e})^{n-2}|\mathfrak{z}|^3\\&+\left[\frac{nb(n-1)}{2q(\mathfrak{z})}(|\mathfrak{z}|+\mathfrak{e})^{n-2}+\frac{\left(nb\mathfrak{e}^{n-1}\right)^2}{hq(\mathfrak{z})}\right]\mathfrak{z}^2.\end{aligned} \tag{B.9}$$

On the other hand, we observe that, $\frac{1}{q(\mathfrak{z})}=\frac{1}{[1+b(\mathfrak{z}+\mathfrak{e})^n]h}$. Therefore, when $\mathfrak{z}\ge0$, we have, $\frac{1}{q(\mathfrak{z})}=\frac{1}{[1+b(|\mathfrak{z}|+\mathfrak{e})^n]h}$, and when $\mathfrak{z}\le0$, then $\mathfrak{z}\in(-\mathfrak{e},0]$. Thus, $\frac{1}{q(\mathfrak{z})}\le\frac{1}{h}\le\frac{1+b(2\mathfrak{e})^n}{[1+b(|\mathfrak{z}|+\mathfrak{e})^n]h}$. Consequently, for all $\mathfrak{z}>-\mathfrak{e}$, we have,

$$\frac{1}{q(\mathfrak{z})}\le\frac{1+b(2\mathfrak{e})^n}{[1+b(|\mathfrak{z}|+\mathfrak{e})^n]h}. \tag{B.10}$$

From (B.10) and (B.9), we deduce that

$$\begin{aligned}\frac{|R(\mathfrak{z})|}{\beta(0)}\le&\left[\mathfrak{p}_1\frac{1+(|\mathfrak{z}|+\mathfrak{e})^{n-2}}{1+b(|\mathfrak{z}|+\mathfrak{e})^n}+\mathfrak{p}_2\frac{(|\mathfrak{z}|+\mathfrak{e})^{n-2}|\mathfrak{z}|}{1+b(|\mathfrak{z}+\mathfrak{e})^n}\right]\mathfrak{z}^2\\\le&\left[\mathfrak{p}_1\frac{1+(|\mathfrak{z}|+\mathfrak{e})^{n-2}}{1+b(|\mathfrak{z}|+\mathfrak{e})^n}+\mathfrak{p}_2\frac{(|\mathfrak{z}|+\mathfrak{e})^{n-1}}{1+b(|\mathfrak{z}+\mathfrak{e})^n}\right]\mathfrak{z}^2,\end{aligned}$$

where the positive constants $\mathfrak{p}_1$ and $\mathfrak{p}_2$ are given by:

$$\mathfrak{p}_1=\left[1+b(2\mathfrak{e})^2\right]^n\max\left\{\frac{nb(n-1)}{2h},\frac{\left(nb\mathfrak{e}^{n-1}\right)^2}{h^2}\right\},$$

and, $\mathfrak{p}_2=\frac{((nb)^2(n-1)\mathfrak{e}^{n-1})(1+b(2\mathfrak{e})^n)}{2h^2}$. Next, observe that:

case 1: if $|\mathfrak{z}|+\mathfrak{e}\le1$, then $\frac{1+(|\mathfrak{z}|+\mathfrak{e})^{n-2}}{1+b(|\mathfrak{z}|+\mathfrak{e})^n}\le2$, and, $\frac{(|\mathfrak{z}|+\mathfrak{e})^{n-1}}{1+b(|\mathfrak{z}+\mathfrak{e})^n}\le1$.

case 2: if $|\mathfrak{z}|+\mathfrak{e}>1$, then $\frac{1+(|\mathfrak{z}|+\mathfrak{e})^{n-2}}{1+b(|\mathfrak{z}|+\mathfrak{e})^n}\le\bar{b}$, and, $\frac{(|\mathfrak{z}|+\mathfrak{e})^{n-1}}{1+b(|\mathfrak{z}+\mathfrak{e})^n}\le\bar{b}$,

where, $\bar{b}=\max\{1,\frac{1}{b}\}$. Therefore, in both cases, we proved that:

$$|R(\mathfrak{z})|\le\mathfrak{m}\mathfrak{z}^2, \tag{B.11}$$

where, $\mathfrak{m}=\beta(0)\max\{\mathfrak{p}_1\max\{2,b^{-1}\},\mathfrak{p}_2\bar{b}\}$.

Now, recall that $R(\mathfrak{z})=\beta(0)[\rho^\dagger(\mathfrak{z})-\frac{\theta}{\beta(0)}\mathfrak{z}]$. From (B.11), we get,

$$\frac{|\beta(0)\rho^\dagger(\mathfrak{z})-\theta\mathfrak{z}|}{|\mathfrak{z}|}\le\mathfrak{m}|\mathfrak{z}|. \tag{B.12}$$

Therefore, we observe that if $|\mathfrak{z}|\le1$, the inequality (B.12) implies that

$$|\beta(0)\rho^\dagger(\mathfrak{z})-\theta\mathfrak{z}|\le\mathfrak{m}|\mathfrak{z}|. \tag{B.13}$$

From (B.2) and (B.13), we conclude that, for all $\mathfrak{z}>-\mathfrak{e}$ and $\mathfrak{e}>0$, we have,

$$|R(\mathfrak{z})|\le\mathfrak{s}|\mathfrak{z}|, \tag{B.14}$$

where $\mathfrak{s}=\max\{\mathfrak{m},2\beta(0)+|\theta|\}$.

Finally, based on (B.11), (B.14) and similar results for $\tilde{R}$, one can easily determine constants $\mathfrak{c}_i$ so that (39) and (40) are satisfied.

Appendix C. Subsequent steps in the proof of Theorem 2

Now, we focus on the function H, defined after (59). We recall that there exist $\mathfrak{c}_i>0$, $i=1,\dots,6$ such that (39) and (40) are satisfied. In addition, from the expression of $V\dagger$, defined in (53), we notice that since $\lambda_1=2$, we get,

$$V^\dagger(X_t,\tilde{X}_t,\tilde{U}_t)\ge\frac{\mathfrak{c}_1}{\max\{\mathfrak{c}_1,\mathfrak{c}_2\}}Q(X(t))+\frac{\mathfrak{c}_2}{\max\{\mathfrak{c}_1,\mathfrak{c}_2\}}Q(\tilde{X}(t),$$

$$\left|\tilde{X}(t)\right|\le\sqrt{V^\dagger(X_t,\tilde{X}_t,\tilde{U}_t)},\quad\text{and,}\quad|X(t)|\le\sqrt{2V^\dagger(X_t,\tilde{X}_t,\tilde{U}_t)}.$$

By combining the previous inequalities, we get the following upper bound:

$$\begin{aligned}\left|H(X_t,\tilde{X}_t)\right|\le&\nu{V^\dagger}^2(X_t,\tilde{X}_t,\tilde{U}_t)+\mathfrak{c}_5\sqrt{2V^\dagger(X_t,\tilde{X}_t,\tilde{U}_t)}Q(X(t-\tau))\\&+[\lambda_4\mathfrak{c}_1(\mathfrak{a}_4+\mathfrak{a}_2)+\mathfrak{c}_3]\sqrt{2V^\dagger(X_t,\tilde{X}_t,\tilde{U}_t)}Q(X(t))\\&+[\lambda_4\mathfrak{c}_2(\mathfrak{a}_4+\mathfrak{a}_2)+\mathfrak{c}_4]\sqrt{2V^\dagger(X_t,\tilde{X}_t,\tilde{U}_t)}Q(\tilde{X}(t))\\&+\mathfrak{c}_6\sqrt{2V^\dagger(X_t,\tilde{X}_t,\tilde{U}_t)}Q(\tilde{X}(t-\tau)),\end{aligned} \tag{C.1}$$

where, $\nu=\frac{(\mathfrak{d}_1\lambda_4+2(\mathfrak{a}_5\lambda_4)^2)\max\{\mathfrak{c}_1,\mathfrak{c}_2\}^2}{2\mathfrak{d}_1}$. A direct consequence is that the time derivative of $V\dagger$ satisfies for almost all $t\ge0$,

$$\begin{aligned}\dot{V}^\dagger(t)\le&-2\bar{\mathfrak{d}}V^\dagger(X_t,\tilde{X}_t,\tilde{U}_t)-\frac{\mathfrak{d}_1}{2}Q(\tilde{U}(t-\tilde{\tau}))\\&-\left[\bar{\mathfrak{d}}-\nu V^\dagger(X_t,\tilde{X}_t,\tilde{U}_t)\right]V^\dagger(X_t,\tilde{X}_t,\tilde{U}_t)\\&-\left[\frac{\mathfrak{d}_4}{2}-(\lambda_4\mathfrak{c}_2(\mathfrak{a}_4+\mathfrak{a}_2)+\mathfrak{c}_4)\sqrt{2V^\dagger(X_t,\tilde{X}_t,\tilde{U}_t)}\right]Q(\tilde{X}(t))\\&-\left[\mathfrak{d}_2-\mathfrak{c}_5\sqrt{2V^\dagger(X_t,\tilde{X}_t,\tilde{U}_t)}\right]Q(X(t-\tau))\\&-\left[\frac{\mathfrak{d}_5}{2}-(\lambda_4\mathfrak{c}_1(\mathfrak{a}_4+\mathfrak{a}_2)+\mathfrak{c}_3)\sqrt{2V^\dagger(X_t,\tilde{X}_t,\tilde{U}_t)}\right]Q(X(t))\\&-\left[\mathfrak{d}_3-\mathfrak{c}_6\sqrt{2V^\dagger(X_t,\tilde{X}_t,\tilde{U}_t)}\right]Q(\tilde{X}(t-\tau)).\end{aligned} \tag{C.2}$$

Consequently, for all initial conditions belonging to the set

$$\mathcal{B}=\left\{\left(\varphi_X,\varphi_{\tilde{X}},\varphi_{\tilde{U}}\right)\in\mathcal{C}_\tau\times\tilde{\mathcal{C}}_\tau\times\tilde{\mathcal{C}}_{\tilde{\tau}}\ \mid\ V^\dagger\left(\varphi_X,\varphi_{\tilde{X}},\varphi_{\tilde{U}}\right)<\overline{V}^\dagger\right\}, \tag{C.3}$$

where, with an abuse of notation, we consider the spaces of continuous functions: $\mathcal{C}_\tau=\mathcal{C}([-\tau,0],(-x_e,+\infty))$, $\tilde{\mathcal{C}}_\tau=\mathcal{C}([-\tau,0],(-\tilde{x}_e,+\infty))$, and, $\tilde{\mathcal{C}}_{\tilde{\tau}}=\mathcal{C}([-\tilde{\tau},0],(-\tilde{u}_e,+\infty))$, as well as the upper bound: $\overline{V}^\dagger=\min\{\frac{\bar{\mathfrak{d}}}{\nu},u_1^2,u_2^2,u_3^2,u_4^2\}$, where, $u_1=\frac{\mathfrak{d}_4}{8(\lambda_4\mathfrak{c}_2(\mathfrak{a}_4+\mathfrak{a}_2)+\mathfrak{c}_4)}$, $u_2=\frac{\mathfrak{d}_5}{8(\lambda_4\mathfrak{c}_1(\mathfrak{a}_4+\mathfrak{a}_2)+\mathfrak{c}_3)}$, $u_3=\frac{\mathfrak{d}_4}{4\mathfrak{c}_5}$, and, $u_4=\frac{\mathfrak{d}_3}{4\mathfrak{c}_6}$, we finally find that the derivative of the functional $V\dagger$ satisfies:

$\dot{V}^\dagger(t)\le-2\bar{\mathfrak{d}}V^\dagger(X_t,\tilde{X}_t,\tilde{U}_t)$, where $\bar{\mathfrak{d}}>0$, for almost all $t\ge0$.

References

Adimy, M., Chekroun, A., Touaoula, T.M., 2015. Age-structured and delay differential-difference model of hematopoietic stem cell dynamics. Discret. Contin. Dyn. Syst. Ser. B 20 (9), 2765–2791.

Adimy, M., Crauste, F., Abdllaoui, A., 2008. Discrete-maturity structured model of cell differentiation with applications to acute myelogenous leukemia. J. Biol. Syst. 16 (3), 395–424.

Aguirre-Ghiso, J.A., 2006. The problem of cancer dormancy: understanding the basic mechanisms and identifying therapeutic opportunities. Cell Cycle Taylor Francis Online, 5 (6), 1740–1743.

Aguirre-Ghiso, J.A., 2007. Models, mechanisms and clinical evidence for cancer dormancy. Nat. Rev. Cancer 7 (11), 834–846.

Ahsen, M., Özbay, H., Niculescu, S.I., 2015. Analysis of Deterministic Cyclic Gene Regulatory Network Models with Delays, Birkhäuser.

Al-Asadi, M.G., Brindle, G., Castellanos, M., May, S.T., Mills, K.I., Russell, N.H., Seedhouse, C.H., Pallis, M., 2017. A molecular signature of dormancy in $CD34^{+}$ $CD38^{-}$acute myeloid leukaemia cells. Oncotarget Blood. 8 (67), 111405.

Avila, J.L., 2014. A coupled model for healthy and cancerous cells dynamics in acute myeloid leukemia. IFAC Proc. 47 (3), 7529–7534.

Avila, J.L., Bonnet, C., Clairambault, J., Özbay, H., Niculescu, S.I., Merhi, F., Tang, R., Marie, J.P., 2012. A new model of cell dynamics in acute myeloid leukemia involving distributed delays. In: Proceedings of the Tenth IFAC Workshop on Time Delay Systems (TDS), pp. 55–60.

Bélair, J., Mackey, M.C., Mahaffy, J.M., 1995. Age-structured and two-delay models for erythropoiesis. Math. Biosci. 128 (1–2), 317–346.

Bellomo, N., Forni, G., 1994. Dynamics of tumor interaction with the host immune system. Math. Comput. Model. 20 (1), 107–122.

Bernard, S., Bélair, J., Mackey, M.C., 2003. Oscillations in cyclical neutropenia: new evidence based on mathematical modeling. J. Theor. Biol. 223 (3), 283–298.

Brahmer, J.R., Pardoll, J.R., 2013. Immune checkpoint inhibitors: making immunotherapy a reality for the treatment of lung cancer. Cancer Immunol. Res. 1 (2), 85–91.

Brandwein, J.M., 2015. Targeting polo-like kinase 1 in acute myeloid leukemia. Ther. Adv. Hematol. 6 (2), 80–87.

Burns, F.J., Tannock, J.F., 1970. On the existence of a G_0-phase in the cell cycle. Cell Tissue Kinet. 3, 321–334.

Chaffer, C.L., Brueckmann, I., Scheel, C., Kaestli, A.J., Wiggins, P.A., Rodrigues, L.O., Brooks, M., Reinhardt, F., Su, Y., Polyak, K., Arendt, L.M., 2011. Normal and neoplastic nonstem cells can spontaneously convert to a stem-like state. Proc. Natl. Acad. Sci. 108 (19), 7950–7955. (2011).

Colijn, C., Mackey, M.C., 2005. A mathematical model of hematopoiesisl. Periodic chronic myelogenous leukemia. J. Theor. Biol. 237 (2), 117–132.

Crane, G.M., Jeffery, E., Morrison, S.J., 2017. Adult haematopoietic stem cell niches. Nat. Rev. Immunol. 17 (9), 573.

Delhommeau, F., Dupont, S., Della Valle, V., James, C., Trannoy, S., Massé, A., Kosmider, O., Le-Couedic, J.P., Robert, F., Alberdi, A., Lécluse, Y., Plo, I., Dreyfus, F.J., Marzac, C., Casadevall, N., Lacombe, C., Romana, S.P., Dessen, P., Soulier, J., Viguié, F., Fontenay, M., Vainchenker, W., Bernard, O.A., 2009. Mutation in TET2 in myeloid cancers. New Engl. J. Med. 360 (22), 2289–2301.

Djema, W., Mazenc, F., Bonnet, C., 2016a. Analysis of a nonlinear delay differential-difference biological model. IFAC-PapersOnLine, IFAC Conf. Time-Delay Syst. 49 (10), 246–251.

Djema, W., Mazenc, F., Bonnet, C., 2017a. Stability analysis and robustness results for a nonlinear system with distributed delays describing hematopoiesis. In: Systems & Control Letters, 102. Elsevier, pp. 93–101.

Djema, W., Mazenc, F., Bonnet, C., Clairambault, J., Hirsch, P., Delhommeau, F., 2016b. Stability of a delay system coupled to a delay differential-difference system describing the coexistence of ordinary and mutated hematopoietic stem cells. In: Proceedings of the Fifty-Fifth Conference on Decision and Control. Las Vegas, USA.

Djema, W., Mazenc, F., Bonnet, C., Clairambault, J., Hirsch, P., Delhommeau, F., 2017b. Analysis of a model of dormancy in cancer as a state of coexistence between tumor and healthy stem cells. In: Proceedings of the American Control Conference. Seattle, USA.

Döhner, H., Weisdorf, D.J., Bloomfield, C.D., 2015. Acute myeloid leukemia. New Engl. J. Med. 373, 1136–1152.

Ebinger, S., Özdemir, E.Z., Ziegenhain, C., Tiedt, S., Alves, C.C., Grunert, M., Dworzak, M., Lutz, C., Turati, V.A., Enver, T., Horny, H.P., 2016. Characterization of rare, dormant, and therapy-resistant cells in acute lymphoblastic leukemia. Cancer Cell 30 (6), 849–862.

Eftimie, R., Bramson, J.L., Earn, D.J., 2011. Interactions between the immune system and cancer: a brief review of non-spatial mathematical models. Bull. Math. Biol. 73 (1), 2–32.

Enderling, H., 2013. Cancer stem cells and tumor dormancy. In: Systems Biology of Tumor Dormancy. Springer, NY, pp. 55–71.

Fang, Y., Zhong, L., Lin, M., Zhou, X., Jing, H., Ying, M., Luo, P., Yang, B., He, Q., 2013. MEK/ERK dependent activation of STAT1 mediates dasatinib-induced differentiation of acute myeloid leukemia. PLoS One 8 (6), p. e66915.

Ferrarini, M., Ferrero, E., Dagna, L., Poggi, A., Zocchi, M.R., 2002. Human T cells: a nonredundant system in the immune-surveillance against cancer. Trends Immunol. 23 (1), 14–18.

Feuring-Buske, M., Frankel, A.E., Alexander, R.L., Gerhard, B., Hogge, D.E., 2002. A diphtheria toxin-interleukin 3 fusion protein is cytotoxic to primitive acute myeloid leukemia progenitors but spares normal progenitors. Cancer Res. 62 (6), 1730–1736.

Foley, C., Bernard, S., Mackey, M.C., 2006. Cost-effective G-CSF therapy strategies for cyclical neutropenia: mathematical modelling based hypotheses. J. Theor. Biol. 238 (4), 754–763.

Foley, C., Mackey, M.C., Math, J., 2009. Dynamic hematological disease: a review. J. Math. Biol. 58 (1–2), 285–322.

Folkman, J., Kalluri, R., 2004. Cancer without disease. Nature 427 (6977), 786–787.

Fridman, E., 2002. Stability of linear descriptor systems with delay: a Lyapunov-based approach. J. Math. Anal. Appl. 273 (1), 24–44.

Fridman, E., 2014. Introduction to time-delay systems: analysis and control. Systems and Control: Foundations and Applications. Birkhauser.

Fridman, E., Bonnet, C., Mazenc, F., Djema, W., 2016. Stability of the cell dynamics in acute myeloid leukemia. Syst. Control Lett. 88, 91–100.

Gatenby, R.A., 2009. A change of strategy in the war on cancer. Nature 459 (7246), 508–509.

Godwin, C.D., Gale, R.P., Walter, R.B., 2017. Gemtuzumab ozogamicin in acute myeloid leukemia. Leukemia 31 (9), 1855.

Gu, K., Liu, Y., 2009. Lyapunov–Krasovskii functional for uniform stability of coupled differential-functional equations. Automatica 45 (3), 798–804.

Hayden, E.C., 2009. Cutting off cancer's supply lines. Nature 458 ((7239), 686–687.

Hirsch, P., Zhang, Y., Tang, R., Joulin, V., Boutroux, H., Pronier, E., Moatti, H., Flandrin, P., Marzac, C., Bories, D., Fava, F., 2016. Genetic hierarchy and temporal variegation in the clonal history of acute myeloid leukaemia. Nat. Commun. 7, 12475.

Hoffman, R., Benz, E.J., Silberstein, L.E., Heslop, H., Weitz, J., Anastasi, J., 2012. Hematology: Basic Principles and Practice, sixth ed. Elsevier, Churchill Livingstone.

Hollstein, M., Sidransky, D., Vogelstein, B., Harris, C.C., 1991. P53 mutations in human cancers. Science 253 (5015), 49–53.

Jansen, G., Gatenby, R., Aktipis, C.A., 2015. Control vs. eradication: applying infectious disease treatment strategies to cancer. Proc. Natl. Acad. Sci. U.S.A. 112 (4), 937–938.

Jordan, C.T., Guzman, M.L., Noble, M., 2006. Cancer stem cells. New Engl. J. Med. 355 (12), 1253–1261.

Karafyllis, I., Pepe, P., Jiang, Z.P., 2009. Stability results for systems described by coupled retarded functional differential equations and functional difference equations. Nonlinear Anal. Theory Methods Appl. 71, 3339–3362.

Kareva, I., 2016. Primary and metastatic tumor dormancy as a result of population heterogeneity. Biol. Direct 11 (1), 37.

Keener, J.P., Sneyd, J., 2009. Mathematical Physiology, 1. Springer, New York.

Lainey, E., Thépot, S., Bouteloup, C., Sébert, M., Adès, L., Tailler, M., Gardin, C., Botton, S., Baruchel, A., Fenaux, P., Kroemer, G., Boehrer, S., 2011. Tyrosine kinase inhibitors for the treatment of acute myeloid leukemia: delineation of anti-leukemic mechanisms of action. Biochem. Pharmacol. 82, 1457–1466.

Langer, C.J., 2015. Emerging immunotherapies in the treatment of nonsmall cell lung cancer (NSCLC): the role of immune checkpoint inhibitors. Am. J. Clin. Oncol. 38 (4), 422–430.

Mackey, M.C., 1978. Unified hypothesis of the origin of aplastic anemia and periodic hematopoiesis. Blood 51, 941–956.

Mackey, M.C., Pujo-Menjouet, L., Wu, J., 2006. Periodic oscillations of blood cell populations in chronic myelogenous leukemia. SIAM J. Math. Anal. 38 (1), 166–187.

Marciniak-Czochra, A., Stiehl, T., Ho, A.D., Jäger, W., Wagner, W., 2009. Modeling of asymmetric cell division in hematopoietic stem cellsregulation of self-renewal is essential for efficient repopulation. Stem Cells Dev. 18 (3), 377–386.

McKendrick, A.G., 1925. Applications of mathematics to medical problems. Proc. Edinb. Math. Soc. 44, 98–130.

Michel, A.N., Hou, L., Liu, D., 2015. Stability of dynamical systems: continuous, discontinuous, and discrete systems. Systems & Control: Foundations & Applications, second Birkhäuser.

Morgan, D., 2006. The cell cycle: principles of control. In: Primers in Biology Series. Oxford University Press, p. 297.

Naumov, G.N., Folkman, J., Straume, O., 2009. Tumor dormancy due to failure of angiogenesis: role of the microenvironment. Clin. Exp. Metast. 26 (1), 5160.

Nielsen, M., Thomsen, J., Primdahl, S., Dyreborg, U., Andersen, J., 1987. Breast cancer and atypia among young and middle-aged women: a study of 110 medicolegal autopsies. Br. J. Cancer 56 (6), 8149.

Özbay, H., Bonnet, C., Benjelloun, H., Clairambault, J., 2012. Stability analysis of cell dynamics in leukemia. Math. Model Nat. Phenom. 7 (1), 203–234.

Pardoll, D.M., 2012. The blockade of immune checkpoints in cancer immunotherapy. Nat. Rev. Cancer 12 (4), 252.

Passegué, E., Jamieson, C.H., Ailles, L.E., Weissman, I.L., 2003. Normal and leukemic hematopoiesis: are leukemias a stem cell disorder or a reacquisition of stem cell characteristics? Proc. Natl. Acad. Sci. Regenerative Medicine U.S.A. 100 (Suppl 1), 11842–11849.

Pepe, P., 2003. The liapunov's second method for continuous time difference equations. Int. J. Robust Nonlinear Control 13 (15), 1389–1405.

Preziosi, L., 1996. From population dynamics to modelling the competition between tumors and immune system. Math. Comput. Model. 23 (6), 135–152.

Pronier, E., Delhommeau, F., 2011. Inhibition of TET2-mediated conversion of 5-methylcytosine to 5-hydroxymethylcytosine disturbs erythroid and granulomonocytic differentiation of human hematopoietic progenitors. Blood 118 (9), 2551–2555.

Pujo-Menjouet, L., 2016. Blood cell dynamics: half of a century of modelling. Math. Model. Nat. Phenom. 11 (1), 92–115.

Pujo-Menjouet, L., Bernard, S., Mackey, M.C., 2005. Long period oscillations in a G_0 model of hematopoietic stem cells. SIAM. J. Appl. Dyn. Syst. 4 (2), 312–332.

Qian, H., 2012. Cooperativity in cellular biochemical processes: noise-enhanced sensitivity, fluctuating enzyme, bistability with nonlinear feedback, and other mechanisms for sigmoidal responses. Ann. Rev. Biophys. 41, 179–204.

Reya, T., Morrison, S.J., Clarke, M.F., Weissman, I.L., 2001. Stem cells, cancer, and cancer stem cells. Nature 414 (6859), 105–111.

Reynolds, A.R., 2009. Stimulation of tumor growth and angiogenesis by low concentrations of RGD-mimetic integrin inhibitors. Nat. Med. 15 (4), 392–400.

Rowe, J.M., Löwenberg, B., 2013. Gemtuzumab ozogamicin in acute myeloid leukemia: a remarkable saga about an active drug. Blood 121 (24), 4838–4841.
Saygin, C., Carraway, H.E., 2017. Emerging therapies for acute myeloid leukemia. J. Hematol. Oncol. 10 (1), 93.
Schreiber, R.D., Old, L.J., Smyth, M.J., 2011. Cancer immunoediting: integrating immunity's roles in cancer suppression and promotion. Science 331 (6024), 1565–1570.
Smith, J.A., Martin, L., 1973. Do cells cycle? Proc. Natl. Acad. Sci. 70 (4), 1263–1267.
Stiehl, T., Marciniak-Czochra, A., 2011. Characterization of stem cells using mathematical models of multistage cell lineages. Math. Comput. Model. 53 (7), 1505–1517.
Stiehl, T., Marciniak-Czochra, A., 2012. Mathematical modeling of leukemogenesis and cancer stem cell dynamics. Math. Model. Nat. Phenom. 7 (1), 166–202.
Stone, R.M., Mandrekar, S.J., Sanford, B.L., Laumann, K., Geyer, S., Bloomfield, C.D., Thiede, C., Prior, T.W., Döhner, K., Marcucci, G., Lo-Coco, F., 2017. Midostaurin plus chemotherapy for acute myeloid leukemia with a FLT3 mutation. New Engl. J. Med 377 (5), 454–464.
Sykes, D.B., Kfoury, Y.S., Mercier, F.E., Wawer, M.J., Law, J.M., Haynes, M.K., Lewis, T.A., Schajnovitz, A., Jain, E., Lee, D., Meyer, H., 2016. Inhibition of dihydroorotate dehydrogenase overcomes differentiation blockade in acute myeloid leukemia. Cell 167 (1), 171–186.
Thieme, H.R., 2003. Mathematics in population biology. Princeton Series in Theoretical and Computational Biology. Princeton University Press.
Tuch, B., 2006. Stem cells – a clinical update. Aust. Fam. Physician 35 (9), 719.
Uhr, J.W., Scheuermann, R.H., Street, N.E., Vitetta, E.S., 1997. Cancer dormancy: opportunities for new therapeutic approaches. Nat. Med. 3 (5), 505–509.
Vesely, M.D., 2011. Natural innate and adaptive immunity to cancer. Ann. Rev. Immunol. 29, 235–271.
Wake, G.C., 2003. The solution and the stability of a nonlinear age-structured population model. ANZIAM J. 45 (02), 153–165.
Wilkie, K.P., Hahnfeldt, P., 2013. Tumorimmune dynamics regulated in the microenvironment inform the transient nature of immune-induced tumor dormancy. J. Cancer Res. 73 (12), 353444.
Zarrinkar, P.P., 2009. AC220 is a uniquely potent and selective inhibitor of FLT3 for the treatment of acute myeloid leukemia (AML). Blood 114 (14), 2984–2992.
Zitvogel, L., Apetoh, L., Ghiringhelli, F., Kroemer, G., 2008. Immunological aspects of cancer chemotherapy. Nat. Rev. Immunol. 8 (1), 58–73.
Zitvogel, L., Tesniere, A., Kroemer, G., 2006. Cancer despite immunosurveillance: immunoselection and immunosubversion. Nat. Rev. Immunol. 6 (10), 715–727.